Hindawi
Applied Bionics and Biomechanics
Volume 2023, Article ID 9169050, 27 pages
https://doi.org/10.1155/2023/9169050

Research Article

Estimation of the Angles of a Robotic Arm with 7-Free Degrees Using an Improved Hybrid ESSA Algorithm

Inayet Hakki Cizmeci [1] **and Adem Alpaslan Altun** [2]

[1]*Akseki Vocational School, Computer Technologies, Alanya Alaaddin Keykubat University, Antalya 07425, Turkey*
[2]*Faculty of Technology Computer Engineering, Selcuk University, Konya 42100, Turkey*

Correspondence should be addressed to Inayet Hakki Cizmeci; inayet.cizmeci@alanya.edu.tr

Received 30 November 2022; Revised 29 May 2023; Accepted 5 June 2023; Published 14 August 2023

Academic Editor: Liwei Shi

The electro-search algorithm (ESO) encounters challenges arising from its slow convergence rate and propensity to descend into local optima. In this study, a hybrid variant based on simulated annealing (SA), termed electro search simulated annealing (ESSA), is proposed to tackle these issues and surmount the obstacles. SA assists the proposed ESSA in escaping local optima through the cooling process while propelling individuals within the population. As these propelled individuals search for new positions, they engage in exploration and consequently approach the global optimum. This establishes a balance between exploitation and exploration for ESSA. ESSA has been compared with 10 metaheuristic algorithms on 15 benchmark functions with dimensions of 100, 500, and 1,000. The experimental results demonstrate its high-solution accuracy. Moreover, ESSA has been tested in the optimization of a robotic arm, a technology that requires low-error rates in the medical field. The analysis reveals the competitiveness and advantages of the proposed ESSA algorithm.

1. Introduction

Metaheuristic algorithms are methods derived from natural phenomena or physical and social rules that are employed to solve complex optimization problems. These algorithms explore the problem space through nonstatic heuristic processes, generating suitable solutions. They typically adopt nongradient-based approaches. Metaheuristic frameworks offer flexible and robust algorithmic structures that can be adapted to various optimization problems and customized to specific problems with only a few modifications [1, 2]. In real-world optimization problems, the search space expands exponentially, and the problem perspective changes multidimensionally, often leading to standard optimization methods' inability to produce optimal solutions. Real-world problems are generally nonlinear and constrained in structure. Therefore, metaheuristic algorithms are required for solving multidimensional real-world problems [3–5]. A multidimensional optimization problem can be expressed as a minimization problem in d dimensions Equation (1).

$$\begin{aligned} &\min F(X), \\ &X = \left[x_{i,d}\right], \ \text{lower} \le x \le \text{upper}. \end{aligned} \tag{1}$$

Here, $\left[x_{i,d}\right]$ represents the decision vector, $F(X)$ denotes the fitness function, and lower $\le x \le$ upper indicates the range of the variable x. These algorithms, focused on exploring vast and complex search spaces, increase the probability of finding the best global solution. However, there is no guarantee of finding a global solution. As the number of dimensions increases, the likelihood of the algorithm getting stuck on the local best solutions also increases. Additionally, the computation time will significantly increase [6]. This situation negatively impacts the algorithm's performance. When employing hybrid approaches in optimization processes, it is crucial to maintain a balance between exploitation and exploration activities. Successfully achieving this balance significantly improves the search efficiency. In general, solutions with high-fitness values exhibit better development performance, while solutions with low-fitness values possess the potential to preserve population diversity and strengthen

search capabilities. By employing a hybrid approach, the algorithm's exploration efficiency can be enhanced by directing individuals during the exploration phase while attempting to escape the exploitation phase [7]. There are studies on hybrid metaheuristic algorithms in the literature. Some of these studies are as follows:

Optimization of proportional–integral–derivative (PID) control systems used in automobile cruise control systems [8], solutions to nonlinear or linearized problems [9], design of PID control systems used in automatic voltage regulator (AVR) systems [10], function optimization of buck converter systems, and achieving efficient controller design [11], design of the control mechanism for a functional electrical stimulation (FES) system [12], design of an efficient controller for a vehicle cruise control system [13], solving nonlinear multidomain economic dispatch problems [14], parameterization of solar photovoltaic models [15], uncertainty-based dynamic economic dispatch for various load and wind profiles [16], and cognitive radio models for agricultural applications [17].

Various hybrid algorithms can be found in the literature, such as the enhanced particle swarm optimization algorithm (e-mPSOBSA), which possesses the advantages of both particle swarm optimization (PSO) and backtracking search algorithm (BSA) [18]; the hybrid SMA (HSMA) algorithm, which combines the slime mold algorithm (SMA) and quadratic approximation (QA) [19]; the hybrid sine cosine butterfly optimization algorithm (BOA), in which a modified BOA is combined with a sine cosine algorithm [20]; a new hybrid metaheuristic algorithm that integrates the BOA with the Moth-flame optimization (MFO) algorithm, termed h-MFOBOA [21]; and a new hybrid evolutionary algorithm (SHADE-WOA) that merges the success history-based adaptive differential evolution (SHADE) and the modified whale Optimizer (WOA) algorithms [22].

Several applications of the simulated annealing (SA) algorithm can be found in hybrid approaches. Some of these include: the hybridization of the Harris Hawks optimization (HHO) and SA techniques for automatic voltage regulator (AVR) control [23]; the combination of Lévy flight distribution and SA algorithms to achieve optimal parameterization of the fractional-order proportional-integral-derivative (FOPID) controller [24]; and the integration of Manta ray foraging optimization (MRFO) with SA algorithms to adjust the parameters of the FOPID controller for controlling the speed of direct current (DC) motors [25].

Metaheuristic algorithms are generally inspired by nature [26]. Some of these algorithms include PSO [27], atom search algorithm (ASO) [28], bacterial foraging optimization (BFO) [29], grey wolf optimizer (GWO) [30], ant colony optimization (ANT) [31], artificial bee colony (ABC) [32], genetic algorithm (GA) [33], farmland fertility algorithm (FFA) [34], African vulture optimization algorithm (AVOA) [35], artificial gorilla troop optimization algorithm (GTO) [36], mountain gazelle optimizer (MGO) [37], chimp optimization algorithm (ChOA) [38], multiple trial differential evolution algorithm (DMDE) [39], cross-dimensional coordination gray wolf optimizer (CDCGWO) [40].

In this study, a hybrid electro search simulated annealing (ESSA) algorithm is proposed, combining the SA algorithm [41], which can escape the local exploitation stage, with the successful electro-search algorithm (ESO) [42] during the exploration stage.

Nowadays, robotic arm technology is used in many areas of industry. Robotic arms are defined as serial manipulators with high degrees of freedom (DOF), depending on their usage purposes. The end effector must be precisely positioned at the desired location. To achieve this, the joint angles of the robotic arm must be calculated using kinematic analysis [43]. Particularly in surgeries, the positioning error rates of robotic arms must be very low. Metaheuristic algorithms are used to calculate the arm angles easily and accurately. Some studies in the literature that focus on a high DOF for serial manipulators using metaheuristic algorithms are as follows: Ayyıldız and Çetinkaya devised a serial motor manipulator with 4-DOF. This design employed GA, PSO, quantum particle swarm (QPSO), and gravity search methods to solve the inverse kinematic issue. They demonstrated the significant effect of QPSO on the solution [44]. Vaishnavi et al. [45] used 14 metaheuristic algorithms to calculate angles for the 5-DOF manipulators. The gray wolf algorithm was found to have the best computation time [45]. Rokbani et al. [46] investigated the solution of the inverse kinematics of the 5-DOF robotic arm by modifying the PSO algorithm. Hasan et al. [47] proposed a learning strategy using an artificial neural network to control a serial manipulator with 6-DOF. Nyong and Marttyns developed a 6-DOF robotic arm for welding oil and gas lines. Grey wolf, advanced gray wolf, PSO, jellyfish, and whale optimization algorithms were used to solve the inverse kinematic problem. The performances of these algorithms were compared [48]. Dereli and Kokler used the PSO algorithm with quantum behavior to solve the inverse kinematics of a serial manipulator with 7-DOF. They compared it with other metaheuristic algorithms according to computation times, the number of iterations, and the number of particles [49]. Nguyen et al. [50] used PSO, the differential evolution algorithm (DE), and improved DE and PSO algorithms for the inverse kinematic solution of the 7-DOF serial manipulator. They used two different tip-effector motions in performance comparisons. Aiming to solve only the inverse kinematics problems of 7–8 DOF manipulators, Alexis et al. [51] proposed that the PSO algorithm can also be used in trajectory planning.

The proposed metaheuristic ESSA algorithm has been used for the kinematic analysis of a serial manipulator with 7-DOF. As a result of the analysis, the error rates in reaching the determined positions for the end effector were found to be zero. The proposed ESSA algorithm demonstrated better performance than PSO, GWO, GA, ESO, ASO, ANT, and ABC algorithms. Moreover, the efficiency of the ESSA algorithm was investigated on 15 well-known test functions, and the results were compared with other metaheuristic algorithms. The comparisons revealed its superior ability to achieve solution accuracy. This shows that the algorithm can provide promising and occasionally competitive results. The main contributions of this study are as follows:

(1) ESSA has been proposed to improve convergence speed and solution accuracy in optimization problems compared to ESO.

(2) Enhancing the exploration ability of ESSA has been targeted. The local exploitation ability of SA and the exploration ability of ESO have been combined. This way, a balance has been established between exploitation and exploration, improving overall capability.
(3) The superiority of the ESSA algorithm in terms of problem-solving ability compared to other algorithms has been investigated on 15 well-known unimodal and multimodal benchmark functions with dimensions of 100, 500, and 1,000.
(4) As a result of the kinematic analysis performed with the ESSA algorithm, the error rates in reaching the determined positions for the end effector were found to be zero, and the advantages over other metaheuristic algorithms were revealed.
(5) It has been shown that the ESSA algorithm can occasionally provide better, and more competitive results compared to other metaheuristic algorithms. This demonstrates the potential of the ESSA algorithm as an effective tool for real-world optimization problems and robotic arm kinematic analysis.

The organizational structure of the paper is as follows: Section 2 describes the principle of SA and ESO. The proposed ESSA is presented in Section 3. In Section 4, an analysis is performed that involves comparing the ESSA algorithm with other algorithms and evaluating the outcomes of the experiments. In Section 5, the ESSA algorithm is applied to solve the kinematic analysis of a 7-DOF serial manipulator. Finally, the conclusion and future work are included in Section 6.

2. Algorithms

2.1. Simulated Annealing Algorithms. The SA algorithm was proposed by Kirkpatrick et al. [52]. They observed a similarity between the physical annealing of solids and combinatorial optimization problems. The fundamental principle is that the solid is slowly cooled to reach the low-energy ground state. The general structure of the algorithm allows it to search for the global minimum by moving away from the local minimum [53]. The pseudocode of the SA Algorithm 1 is as follows:

Swaps alter the positions of two elements in a randomly selected sequence within the solution set. T denotes the temperature control, TempFactor represents the cooling coefficient, T_0 signifies the initial temperature, and S_0 corresponds to the initial solution. Next, $e^{-\Delta/T}$ generates a random value to determine the acceptance or rejection of the new solution space. This generated value lies within the range [0, 1]. Finally, the new solution space is accepted if it is greater than or equal to the randomly generated number [54].

2.2. Electro-Search Algorithm. The ESO algorithm is inspired by the Bohr atomic model. It is based on the principle of electron displacement in orbits around the atomic nucleus. As a result of the movement of electrons in their orbits, they emit or absorb energy, which is explained by the Rydberg formula Equation (2):

Input: Initial solution S_0, array Swaps, doubles T_0, *TempFactor*, *FinalTemp*, integer *NInnerLoopIters*
Output: Solution S
$S \leftarrow S_0$, $T \leftarrow T_0$
While $T >$ FinalTemp **do**
  iter $\leftarrow 0$;
  While iter < NInnerLoopIters **do**
    irandom $\leftarrow$ floor(random(0, 1) $*$ Swap.length);
  $S^{\iota} \leftarrow$ ApplySwap[Swaps[iRandom], S,);
  $\Delta \leftarrow c(S^{\iota}) - c(S)$;
  prob $\leftarrow 1, e^{-\frac{\Delta}{T}}$
  if $\Delta < 0$
    $S \leftarrow S^{\iota}$;
  else
    if random $(0, 1) \leq$ prob **then**
      $S \leftarrow S^{\iota}$;
    End
  End
  iter $\leftarrow$ iter $+ 1$;
  EndWhile
$T \leftarrow$ TempFactor $* T$
EndWhile

Algorithm 1: SA Algorithms for procedure code.

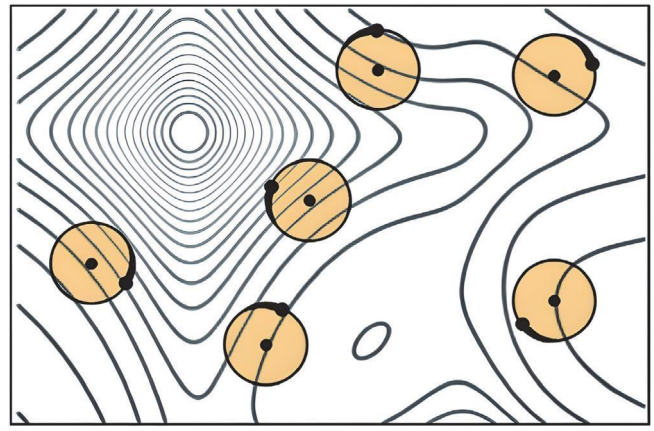

Figure 1: Atom spreading [42].

$$\frac{1}{\lambda} = R \cdot \left(\frac{1}{n_f^2} - \frac{1}{n_i^2}\right), \tag{2}$$

λ denotes the wavelength, n_f represents the final energy level, and n_i signifies the energy level of the transition electron [55].

2.2.1. Atom Spreading. Randomly created atoms are scattered in the defined region as shown in Figure 1. Atoms possess nuclei and orbits where electrons may be placed. These electrons travel toward orbits with higher energy levels [42].

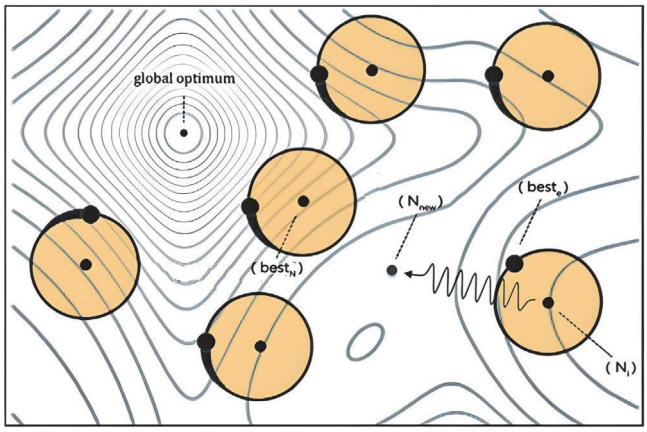

FIGURE 2: Nucleus displacement [55].

2.3. Orbit Transfer. The energy level of the electrons around each nucleus wants to move to the higher orbitals. The quantized energy concept of the hydrogen atom inspires this. The position of the electron for each nucleus is given in Equation (3) [42].

$$e_i = N_i + (2 \times \text{rand} - 1)\left(1 - \frac{1}{n^2}\right) r \quad \text{rand}\,[0,\ 1] \qquad n \in \{2,\ 3,\ 4,\ 5\}, \tag{3}$$

here, e_i is the electron's position, N_i is the current atom and is a generated number between 0 and 1, n is the number of orbitals, and r is the orbital radius [42].

2.3.1. Nucleus Displacement. The distances from each nucleus in the population to the best position are calculated with Equation (4). Equation (5) is employed to execute the movement toward the best position as shown in Figure 2.

$$\overrightarrow{D_k} = \left(\overrightarrow{e}_{best} - \overrightarrow{N}_{best}\right) + Re_k \otimes \left(\frac{1}{\overrightarrow{N}^2_{best}} - \frac{1}{\overrightarrow{N}^2_{k}}\right), \tag{4}$$

$$\overrightarrow{N}_{new} = \overrightarrow{N}_k - Ac_k x \overrightarrow{D}_k, \tag{5}$$

$\overrightarrow{e}_{\text{best}}$ is the best position vector of the nucleus, $\overrightarrow{D_k}$ is the displacement distance of each nucleus, $\overrightarrow{N}_{\text{best}}$ is the best position of the current atom, $\overrightarrow{N}_{\text{new}}$ is the new position vector of the nucleus, and k is the number of iterations. *Re* and *Ac* are convergence coefficients. They affect the performance of the algorithm. The classical ESO algorithm calculates these coefficients using the orbital tuner method. The formula for this method is given in Equations (6) and (7) [42].

$$Re_{k+1} = Re_k + \left(Re_{\text{best}} + \sum_{i=1}^{j} \frac{Re_i/f_{Ni}||Re_i}{1/f_{Ni}||Re_i}\right)/2, \tag{6}$$

$$Ac_{k+1} = Ac_k + \left(Ac_{\text{best}} + \sum_{i=1}^{j} \frac{Ac_i/f_{Ni}||Ac_i}{1/f_{Ni}||Ac_i}\right)/2. \tag{7}$$

Where j is the number of population, k is the number of iteration, Re_k and Ac_k are the algorithm coefficients, $f_{Ni}|Re_i$ and $f_{Ni}|Ac_i$ indicate the nuclei fitness function values, and Re_{best} and Ac_{best} indicate the values of the algorithm coefficients at the best position [42].

3. Proposed Hybrid ESSA Algorithm

Metaheuristic algorithms are designed to identify the optimal region within the search space and guide the process toward the best solution among the population. Some algorithms demonstrate remarkable capabilities in domain exploration, whereas others are particularly adept at finding solutions. The goal of combining such algorithms is to develop a hybrid algorithm with both high exploration and solution capabilities. The proposed ESSA algorithm integrates the area exploration prowess of the ESO algorithm with the solution direction capability of the SA algorithm, which circumvents local exploitation. As a result, a hybrid algorithm with enhanced capacity is proposed.

In metaheuristic algorithms, parameter values are crucial for convergence speed and solution. These parameters can directly affect the performance of the algorithm. The orbital tuner method, which is self-adjusting, has been used to determine *Re* and *Ac* parameters in the ESO algorithm [42]. In the proposed ESSA algorithm, a single convergence parameter is used instead of the *Re* and *Ac* parameters. The determination of this parameter employs a feedback-based PID control system.

3.1. A Feedback Based PID Control System. PID controllers have been widely used in industries for process control applications for decades. With a history dating back to the 1890s, these controllers maintain their popularity in both process and manufacturing sectors today. Research reveals that approximately 90% of process industries use PID as their primary control method [56].

The PID control system is a type of feedback control system created by combining proportional (P), integral (I), and derivative (D) components. These components measure how an error signal (the difference between the desired value and the actual value) changes over time and use this information to generate a control signal. The proportional (P) component produces a control signal proportional to the magnitude of the error. The integral (I) component measures the total (integral) error over time and adjusts the control signal accordingly. The derivative (D) component measures the rate (derivative) of change of the error and adjusts the control signal based on it. The combined use of these three components is called a PID control system [57]. The formulation of the PID control system is shown in Equations (8) and (9).

$$u(t) = k_p e(t) + k_i \int_0^t e(t)\mathrm{d}t + k_d e(t), \tag{8}$$

$$e(t) = y(t) - \delta(t). \tag{9}$$

In the PID control system, $u(t)$ represents the control input, $e(t)$ denotes control error, k_p is the proportional gain, k_d is the derivative gain, and k_i is the integral gain. The variable y signifies the target input value within the given context, while $\delta(t)$ is the output value at time t [58]. The disadvantages of a PID control strategy for nonlinear systems typically include difficulties in the tuning process and challenges in selecting appropriate and accurate controller parameters [59].

Parameter tuning in a PID control system is a critical step in achieving optimal performance. It involves adjusting the proportional (P), integral (I), and derivative (D) gains to obtain the best system response. Several methods exist for tuning the PID controller parameters, ranging from manual approaches to automated algorithms. Ziegler and Nichols [60] proposed one of the earliest tuning methods, where the controller's ultimate gain and oscillation period are obtained experimentally. This method, known as Ziegler–Nichols tuning, provides a simple and systematic way to determine the PID gains [60]. Another popular approach is the Cohen–Coon method, which is based on the system's first order plus time-delay model. This method offers better performance for systems with significant time delays [61].

In recent years, researchers have developed optimization-based techniques for parameter tuning in PID control systems. These methods employ optimization algorithms, such as GAs, PSO, and SA, to find the optimal PID gains [62–65]. In the ESSA algorithm, PID parameters were determined through trial and error.

$$e_i = 5.9 - h_i, \tag{10}$$

$$\text{error}_{\text{rate}(i)} = e_i - e_{i-1}, \tag{11}$$

$$P_i = k_p \times e_i, \tag{12}$$

$$I = k_i \int_0^i e(i)di, \tag{13}$$

$$I_{i+1} = I_i + k_i \times e_i \times \text{iteration}, \quad \text{if} \begin{cases} I_{i+1} > 3 & \text{then } I_{i+1} = 3 \\ I_{i+1} < 0 & \text{then } I_{i+1} = 0 \end{cases}, \tag{14}$$

$$D_i = k_d e(i) \frac{di}{dt}, \tag{15}$$

$$D_i = \left(k_d \times \text{error}_{\text{rate}(i)}\right) \frac{di}{dt}, \tag{16}$$

$$PID_i = P_i + I_i + D_i, \tag{17}$$

$$h_{i+1} = h_i + \text{PID}_i. \tag{18}$$

The goal value in Equation (10) is 5.9, which was chosen after some trial and error. An overshoot may occur if the ESSA algorithm converges to the target value too soon. On the other hand, the algorithm may occasionally become trapped at a local minimum if it approaches the goal value too slowly. The k_p, k_i, and k_d values were carefully chosen through trial and error to overcome this problem. It was discovered that the k_p, k_i and k_d parameters were 44, 2.2, and 4, respectively. Equations (10)–(18) was used to get the convergence coefficient h, which takes the place of the *Re* and *Ac* coefficients in the method.

$$\overrightarrow{D_k} = \left(\overrightarrow{e}_{\text{best}} - \overrightarrow{N}_{\text{best}}\right) + h_k \bigotimes \left(\frac{1}{\overrightarrow{N}^2_{\text{best}}} - \frac{1}{\overrightarrow{N}^2_k}\right), \tag{19}$$

$$\overrightarrow{N}_{\text{new}} = \overrightarrow{N}_k - h_k \times \overrightarrow{D}_k. \tag{20}$$

3.2. The Structure of ESSA. The procedural code for the suggested ESSA algorithm is provided below (Algorithm 2).

In the *neighbor*() function, neighboring solution candidates are determined. Solution candidates are identified based on Equations (21) and (22) being equal.

$$\Delta x = \frac{\text{Random}(0,\ 1) \times -(\text{up} - \text{low}) \times \text{delta}}{2}, \tag{21}$$

$$N_k = N + \Delta x, \tag{22}$$

where Δx is the amount of change, delta is the range of change, N is the population, and N_k is the new neighboring population. The higher the TempFactor value, the slower the system cools and the closer it gets to the global minimum value. However, this causes the algorithm to take longer to reach the result. Since this study employs a hybrid approach, the TempFactor value was set to 0.3 to reach the correct result quickly. The flow diagram of the proposed ESSA algorithm is shown in Figure 3.

3.3. Complexity Analysis

3.3.1. Computational Complexity of ESO. The computational complexity of ESO is determined by specific characteristics such as the size of the nucleus (P), size of electrons (E), dimension (N), and the number of iterations (k). The computational complexity of ESO is as follows:

(1) The generation of the nucleus population: $O\ (P \times N)$.
(2) The generation of the electron population around the nucleus: $O\ (P \times E \times N)$.
(3) Fitness calculation of nucleus: $O\ (P \times N)$.
(4) Fitness calculation of electrons: $O\ (P \times E \times N)$.
(5) Position update nucleus: $O\ (P \times N)$.
(6) Fitness calculation of nucleus during iterations: $O\ (P \times N \times k)$.
(7) Fitness calculation of electrons during iterations: $O\ (P \times E \times N \times k)$.
(8) Update the best solutions during iterations: $O\ (P \times P \times k)$.

1. ***Input:*** $N \rightarrow$ Number of nucleus, $E \rightarrow$ Number of electrons, $Max_{\text{Iteration}} \rightarrow$ Maximum number of iterations, TempFactor $\rightarrow$ Cooling coefficient, $T_0 \rightarrow$ Initialize temp, $Final_{\text{Temp}}$ –> Final temp
2. ***Output:*** Solution N_{best}
3. **for** 1 to N **do**
4. Generate nucleus N,
5. Calculate the fitness value of N,
6. $N_{\text{best}} \leftarrow$ best nucleus of N,
7. **for** 1 to E **do**
8. Generate electron E around nucleus,
9. Calculate the fitness value of E,
10. $E_{\text{best}} \leftarrow$ best nucleus of E,
11. **end for**
12. **end for**
13. **While** Iteration $> Max_{\text{Iteration}}$ **do**
14. **for** $i = 1$ to N
15. Calculate the fitness value of $N_{\text{new}[i]}$,
16. **If** $N_{\text{new}[i]} < N_{\text{best}}$ **then**
17. $N_{\text{best}} \leftarrow N_{\text{new}[i]}$,
18. **end if**
19. **for** $j = 1$ to E
20. Calculate the fitness value of $E_{\text{new}[j]}$,
21. **If** $E_{\text{new}[j]} < E_{\text{best}}$ **then**
22. $E_{\text{best}} \leftarrow N_{\text{new}[j]}$,
23. **end if**
24. **end for**
25. **end for**
26. $T \leftarrow T_0$
27. **While** $T > Final_{\text{Temp}}$ **do**
28. $N_k \rightarrow \text{neighbor}(N)$,
29. $\Delta \leftarrow f(N_k) - f(N_{\text{best}})$,
30. $prob \leftarrow \left(e^{-\frac{\Delta}{T}}\right)$,
31. **If** $\Delta < 0$
32. $N_{best} \leftarrow N_k$,
33. **else**
34. **If** $\text{random}(0, 1) \leq \text{prob}$ **then**
35. $N_{\text{best}} \leftarrow N_k$,
36. **end if**
37. **end if**
38. $T = \text{TempFactor} \times T$,
39. **end While**
40. Iteration = Iteration + 1,
41. **end While**

Algorithm 2: The procedure code of the proposed hybrid ESSA algorithm.

Thus, $O(\text{ESO}) = (k+3)(P \times N) + (k+2)(P \times E \times N) + (P \times P \times k)$.

3.3.2. Computational Complexity of ESSA. The computational complexity of ESSA is determined by P, N, k, and Temp. Temp represents the cooling iteration. Based on the analysis of Algorithm 2, the computational complexity of computing ESSA is as follows:

(1) The generation of the nucleus population: $O(P \times N)$.
(2) The generation of the electron population around the nucleus: $O(P \times E \times N)$.
(3) Fitness calculation of nucleus: $O(P \times N)$.
(4) Fitness calculation of electrons: $O(P \times E \times N)$.
(5) Position update nucleus: $O(P \times N)$.
(6) Fitness calculation of nucleus during iterations: $O(P \times N \times k)$.
(7) Fitness calculation of electrons during iterations: $O(P \times E \times N \times k)$.
(8) The generation of neighbor population during iterations and Temp: $O(P \times N \times k \times Temp)$.
(9) Fitness calculation of neighbor population during iterations and *Temp*Temp: $O(P \times N \times k \times Temp)$.
(10) Update the best solutions during the iterations: $O(P \times P \times k \times Temp)$.

As a result, ESSA's computational complexity:

$$O(\text{ESSA}) = (k+3)(P \times N) + (k+2)(P \times E \times N) + (2 \times P \times N)(P \times k \times Temp). \tag{23}$$

The computational complexity of ESO is lower compared to ESSA. This results in an additional cost for ESSA. However, ESSA's ability to reach the global optimum can partially tolerate this situation.

3.3.3. Space Complexity. The storage space occupied by the algorithm during its operation is the space complexity. The size and dimension of the population determine the space complexity. In ESO and ESSA algorithms, the fundamental space complexity is $O(P \times N)$. The space complexity of ESO and ESSA is the same.

3.4. Advantages of the ESSA Algorithm. The advantages of ESSA are as follows:

(1) ESSA combines the ability of the SA algorithm to escape local exploitation in the problem space with the repulsion of other individuals in the population. This prevents it from falling into a local optimum. On the other hand, ESO tends to fall into local optima.
(2) In ESSA, to reach the correct solution, the algorithm coefficients are updated at each iteration with a PID-based system, increasing the search range. As a result, global exploration capability is enhanced.
(3) While ESSA uses a single parameter to balance exploration and exploitation, ESO employs two distinct parameters, Re and Ac. The Re parameter controls

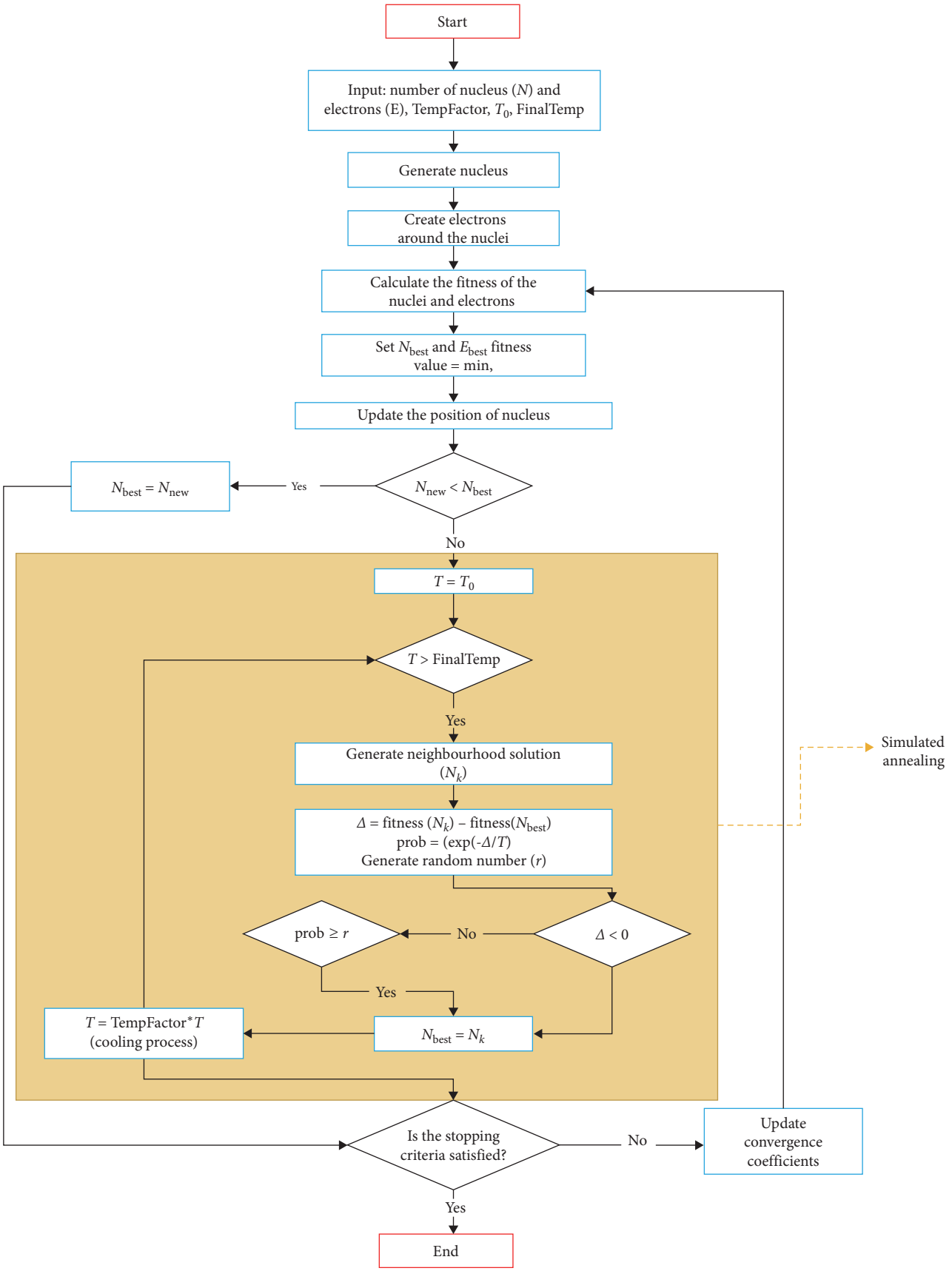

Figure 3: Flow diagram of the proposed ESSA algorithm.

Table 1: Algorithm parameters.

Algorithm	Name of the parameter	Value of the parameter
ESSA	k_p, k_i, k_d	[44, 2.2, 4[
	h (First time random number)	[0, 1]
ESO	*Rei* and *Aci* (algorithm coefficients) (random numbers)	[0, 1]
PSO	C_1 and C_2 (personel and social constants)	2, 2
	w (Inertia weight)	0.8
GWO	a (Area vector)	[0, 2]
ASO	*Alpha* (depth)	50
	Beta (multiplier weight)	0.2
GA	*pmutation* (Mutation probability)	0.5
	pcross (Crossover probability)	0.95

ESSA, electro search simulated annealing.

local exploitation, while the Ac parameter is used for global exploration.

(4) Although ESSA lags other algorithms the average time for solving unimodal functions, it performs almost at the same level in multimodal functions.

4. Results and Discussion

4.1. Experimental Setup and Evaluation Criteria. All algorithms were executed on a computer equipped with Windows 10, an Intel® Core™ Duo E8400 CPU @2.0 GHz, and 6 GB of RAM. The Matlab programing language was used. The performance evaluation was conducted using five criteria: best value, mean, standard deviation (std), ranking, and average time. Further information about these criteria can be found in the study of Daradkeh et al. [66], Liang et al. [67], and Karami and Dariane [68].

(1) *Best value*: the optimal solution discovered by an optimization algorithm.
(2) *Mean*: the average performance of an optimization algorithm across multiple runs.
(3) *Standard deviation*: a measure of the variability in optimization algorithm performance across multiple runs.
(4) *Ranking*: a relative measure comparing the performance of various optimization algorithms.
(5) *Average time*: the average computational time needed for an optimization algorithm to solve a problem.

4.2. Parameter Setting and Benchmark Functions. To evaluate the performance of ESSA in addressing global optimization problems, it was compared to 15 fundamental metaheuristic algorithms, including ABC, PSO, ASO, GA, ESO, GWO, GTO, FFA, AVOA, and MGO. The latter four have recently been proposed as high-performance algorithms. All algorithms were implemented using the parameters reported in the literature, as shown in Table 1. The parameters specific to the ESSA algorithm are detailed in Section 3. Table 2 provides information on benchmark test functions for performance analysis, categorizing them into unimodal (F1–F10) and multimodal (F11–F15) functions. Each algorithm was executed 20 times, and for every run, the best value, mean, standard deviation, ranking, and average time were calculated.

4.3. The Results of Benchmark Functions. Experiments were conducted on 15 benchmark functions with dimensions of 100, 500, and 1,000 and a population size of 20. The results of these experiments are presented in Tables 3–5.

Table 3 displays the results of functions with a dimension of 100. Among these functions, 10 are unimodal (F1–F10), and five are multimodal (F11–F15). For ESSA, the mean and standard deviation values are zero on F1–F5, F7, F9–F10, and F12–F14. Although it does not find the globally optimum value on F6, F11, and F15, ESSA has the closest average and standard deviation values. On the F8 function, the MGO algorithm is the closest to the global optimum point. According to the Friedman test in Table 3, ESSA ranks first in Ave-rank and in total overall rank.

Tables 4 and 5 display the results of analyzing unimodal and multimodal functions with dimensions of 500 and 1,000, respectively. Based on the Friedman test results, ESSA ranks first in Ave-rank values for both unimodal and multimodal functions. Furthermore, it ranks first when considering the functions overall. Despite the increase in dimensions, ESSA performs global exploration without getting trapped in local exploitation. Thus, these analyses indicate that ESSA's performance is superior to that of other algorithms. Figure 4 displays Ave-rank values of 100, 500, and 1,000-dimensional functions for each algorithm.

4.4. Wilcoxon Signed-Rank Test. The Wilcoxon signed-rank test is a nonparametric statistical test used to evaluate comparisons between dependent paired samples. As it operates independently of whether the sample data conforms to a normal distribution, it holds a significant position among nonparametric tests. The Wilcoxon signed-ank test is particularly used to test the median difference between two dependent samples, which is useful in cases of repeated measurements or paired observations in the data set [69]. The application of this test involves ranking the signed differences, ordering them according to their absolute values, and then summing while preserving the signs. The test statistic is based on the difference

Table 2: Benchmark functions.

No	Name	Function	Optima	Range
F1	Sphere	$f(x) = \sum_{i=1}^{n} x_i^2$	0	[−100, 100]
F2	Schwefel 2.22	$f(x) = \sum_{i=1}^{n} \lvert x_i \rvert + \prod_{i=1}^{n} \lvert x_i \rvert$	0	[−10, 10]
F3	Schwefel 1.2	$f(x) = \sum_{i=1}^{n} \left(\sum_{j=1}^{i} x_j \right)^2$	0	[−100, 100]
F4	Schwefel 2.21	$f(x) = \max\{\lvert x_i \rvert, 1 \le i \le n\}$	0	[−100, 100]
F5	Sum square	$f(x) = \sum_{i=1}^{n} i x_i^2$	0	[−5.12, 5.12]
F6	Step	$f(x) = \sum_{i=1}^{n} (x_i + 0.5)^2$	0	[−100, 100]
F7	Quartic	$f(x) = \sum_{i=1}^{n} i x_i^4$	0	[−1.28, 1.28]
F8	Rosenbrock	$f(x) = \sum_{i=1}^{n-1} [100(x_{i+1} - x_i^2)^2 + (x_i - 1)^2]$	0	[−30, 30]
F9	Powell	$f(x) = \sum_{i=1}^{n/k} \left(x_{(4i-3)} + 10x_{(4i-2)}\right)^2 + 5\left(x_{(4i-1)} + x_4 i\right)^2 + \left(x_{(4i-2)} + x_{(4i-1)}\right)^4 + 10\left(x_{(4i-3)} + x_4 i\right)^4$	0	[−4, 5]
F10	Chung Reynold	$f(x) = \sum_{i=1}^{n} (x_i^2)^2$	0	[−100, 100]
F11	Ackley	$f(x) = -a * exp(-b\sqrt{\frac{1}{d}\sum_{i=1}^{d} x_i^2}) - \exp\left(1/d \sum_{i=1}^{d} \cos(cx_i)\right) + a + \exp(1)$	0	[−32.768, 32.768]
F12	Griewank	$f(x) = 1/4000 \sum_{i=1}^{n} x_i^2 - \prod_{i=1}^{n} \cos x_i / \sqrt{i} + 1$	0	[−600, 600]
F13	Salomons	$f(x) = 1 - \cos\left(2\pi\sqrt{\sum_{i=1}^{n} x_i^2}\right) + 0.1\sqrt{\sum_{i=1}^{n} x_i^2}$	0	[−100, 100]
F14	Rastrigin	$f(x) = \sum_{i=1}^{n} x_i^2 - 10 \cos(2\pi x_i) + 10$	0	[−5.12, 5.12]
F15	Alpine	$f(x) = \sum_{i=1}^{n} \lvert x_i \sin(x_i) + 0.1 x_i \rvert$	0	[−10, 10]

between positive and negative ranked sums, and this statistic is compared with an appropriate reference distribution [70].

Tables 6 and 7 display the comparisons between ESSA and other algorithms (ABC, ASO, AVOA, ESO, FFA, GA, GTO, GWO, MGO, and PSO). For each comparison, the p-values and the h-values representing the outcome of the comparisons are provided. Here, all p-values are found to be extremely low and significant ($p < 0.05$). Therefore, it can be concluded that ESSA is statistically significantly different from all other methods. Moreover, the h result value is indicated as "1" for all comparisons, which demonstrates the superiority of ESSA compared to each method.

4.5. Average Execution Time on Benchmark Functions. The convergence speed of ESSA can be evaluated by considering the average execution time. In Tables 3–5, the average time for one iteration is indicated as Ave-time. Three functions of different dimensions have been selected from both unimodal and multimodal functions. The success criterion has been considered in the selection of these functions. The iteration at which the algorithms reached the global optimum point, and the elapsed time are provided in Table 8. Thus, by calculating the total times of the algorithms, information about their convergence speeds has been obtained. According to the calculations, although ESSA lags in unimodal functions in terms of time, it demonstrates good performance in multimodal functions.

5. Application to Engineering Design Problems

5.1. Kinematic Analysis. The mathematical expression representing the structure of a robot manipulator is referred to as kinematic analysis. Two methods are commonly employed in developing this mathematical expression trigonometry and Denavit–Hartenberg (DH) [71]. In this study, the DH method is utilized. The DH method defines the position of each connection point relative to the previous one using four parameters: joint length (t_i), joint offset (d_i), joint angle (θ_i), and joint twist (α_i) [72]. The DH parameters for the 7-DOF robot manipulator in this study are provided in Table 9. The transformation matrix can be derived from Equation (24) [73]. The transformation matrices obtained using the DH parameters are presented in Equations (25–31).

$$A_i = \begin{matrix} \cos\theta_i & -\sin\theta_i \cdot \cos\alpha_i & \sin\theta_i \cdot \cos\alpha_i & t_i \cdot \cos\theta_i \\ \sin\theta_i & \cos\theta_i \cdot \cos\alpha_i & -\cos\theta_i \cdot \sin\alpha_i & t_i \cdot \sin\theta_i \\ 0 & \sin\alpha_i & \cos\alpha_i & d_i \\ 0 & 0 & 0 & 1 \end{matrix}, \tag{24}$$

$$A_1 = \begin{matrix} \cos\theta_1 & 0 & -\sin\theta_1 & t_1 \cdot \cos\theta_1 \\ \sin\theta_1 & 0 & \cos\theta_1 & t_1 \cdot \sin\theta_1 \\ 0 & -1 & 0 & d_1 \\ 0 & 0 & 0 & 1 \end{matrix}, \tag{25}$$

Table 3: Results of unimodal (F1–F10) and multimodal (F11–F15) functions with 100 dimensions.

Function	Criterion	ABC	ASO	AVOA	ESO	ESSA	FFA	GA	GTO	GWO	MGO	PSO
F1	Best	2,46E + 05	1,09E + 03	**0,00E + 00**	2,65E − 12	**0,00E + 00**	6,85E + 01	3,55E + 04	**0,00E + 00**	2,02E − 25	2,15E − 115	**0,00E + 00**
	Mean	2,46E + 05	1,11E + 03	5,68E − 291	2,65E − 12	**0,00E + 00**	1,70E + 03	7,92E + 04	2,21E − 144	1,39E − 16	6,45E − 37	7,27E + 02
	Std	**0,00E + 00**	3,67E + 01	**0,00E + 00**	4,36E − 28	**0,00E + 00**	2,28E + 03	3,51E + 04	5,86E − 144	3,67E − 16	1,71E − 36	9,44E + 02
	Ave-Time (s)	1,81E − 03	2,63E − 03	5,71E − 04	3,88E − 03	9,91E − 03	2,67E − 03	4,83E − 04	7,34E − 04	3,56E − 04	2,17E − 03	3,70E − 04
	Rank	11	8	2	6	**1**	9	10	3	5	4	7
F2	Best	6,35E + 02	6,04E + 01	4,80E − 280	2,99E − 01	**0,00E + 00**	1,38E + 00	1,23E + 02	**0,00E + 00**	3,98E − 15	2,90E − 68	8,00E + 01
	Mean	6,57E + 02	6,19E + 01	6,57E − 138	2,99E − 01	**0,00E + 00**	1,42E + 01	1,24E + 02	3,10E − 84	9,35E − 11	3,89E − 26	8,00E + 01
	Std	3,85E + 01	3,62E + 00	1,74E − 137	0,00E + 00	**0,00E + 00**	1,64E + 01	5,09E + 00	8,21E − 84	2,44E − 10	1,03E − 25	0,00E + 00
	Ave-Time (s)	1,58E − 03	2,51E − 03	4,57E − 04	3,68E − 03	1,02E − 02	2,17E − 03	4,56E − 04	5,56E − 04	3,08E − 04	1,86E − 03	4,24E − 04
	Rank	11	8	2	6	**1**	7	10	3	5	4	9
F3	Best	1,03E + 06	6,92E + 04	**0,00E + 00**	4,32E + 04	**0,00E + 00**	1,92E + 05	6,37E + 04	**0,00E + 00**	1,03E + 01	1,68E − 06	1,13E + 05
	Mean	1,03E + 06	6,94E + 04	1,83E − 166	4,32E + 04	**0,00E + 00**	2,03E + 05	1,01E + 05	9,75E − 142	3,04E + 02	1,44E − 02	1,48E + 05
	Std	1,26E − 10	3,05E + 02	0,00E + 00	0,00E + 00	**0,00E + 00**	2,21E + 04	3,17E + 04	2,58E − 141	5,21E + 02	2,33E − 02	1,94E + 04
	Ave-Time (s)	8,38E − 03	9,53E − 03	2,59E − 03	2,29E − 02	7,27E − 02	1,06E − 02	6,20E − 03	4,38E − 03	2,11E − 03	1,06E − 02	2,25E − 03
	Rank	11	7	2	6	**1**	10	8	3	5	4	9
F4	Best	9,56E + 01	2,20E + 01	3,12E − 276	4,62E + 00	**0,00E + 00**	9,38E + 01	5,87E + 01	**0,00E + 00**	9,53E − 03	1,47E − 41	**0,00E + 00**
	Mean	9,57E + 01	2,20E + 01	3,72E − 127	4,62E + 00	**0,00E + 00**	9,38E + 01	6,53E + 01	6,58E − 84	1,25E − 01	1,19E − 16	**0,00E + 00**
	Std	9,48E − 02	3,76E − 02	9,84E − 127	0,00E + 00	**0,00E + 00**	0,00E + 00	5,08E + 00	1,74E − 83	2,43E − 01	3,14E − 16	**0,00E + 00**
	Ave-Time (s)	1,62E − 03	4,56E − 03	3,53E − 04	3,76E − 03	6,10E − 03	2,09E − 03	3,98E − 04	5,74E − 04	4,31E − 04	2,38E − 03	3,39E − 04
	Rank	11	8	3	7	**1**	10	9	4	6	5	**1**
F5	Best	9,14E + 04	4,58E + 02	**0,00E + 00**	2,89E − 18	**0,00E + 00**	2,18E + 01	3,00E + 03	**0,00E + 00**	1,93E − 26	6,76E − 109	1,20E + 04
	Mean	9,25E + 04	4,76E + 02	6,28E − 285	2,89E − 18	**0,00E + 00**	5,03E + 02	2,94E + 03	8,58E − 164	1,38E − 17	4,50E − 35	1,61E + 04
	Std	3,07E + 03	3,96E + 01	0,00E + 00	0,00E + 00	**0,00E + 00**	6,47E + 02	1,77E + 02	0,00E + 00	3,66E − 17	1,19E − 34	1,95E + 03
	Ave-Time (s)	1,53E − 03	8,20E − 03	3,37E − 04	3,63E − 03	1,01E − 02	2,21E − 03	3,65E − 04	6,10E − 04	3,81E − 04	1,95E − 03	2,94E − 04
	Rank	11	7	2	5	**1**	8	9	3	6	4	10
F6	Best	2,64E + 05	1,01E + 03	7,01E − 05	1,68E + 01	2,22E − 06	4,75E + 01	3,54E + 04	1,14E − 03	1,05E + 01	2,95E − 07	2,39E + 01
	Mean	2,67E + 05	1,02E + 03	9,43E − 04	1,68E + 01	**9,28E − 05**	1,70E + 03	7,94E + 04	9,79E − 02	1,12E + 01	1,33E − 03	3,83E + 02
	Std	3,13E + 03	2,97E + 01	1,01E − 03	0,00E + 00	8,98E − 05	2,29E + 03	3,49E + 04	1,26E − 01	6,91E − 01	2,46E − 03	9,48E + 02
	Ave-Time (s)	1,47E − 03	5,83E − 03	3,73E − 04	3,84E − 03	6,27E − 03	2,23E − 03	4,28E − 04	6,13E − 04	4,83E − 04	1,94E − 03	3,09E − 04
	Rank	11	8	2	6	**1**	9	10	4	5	3	7
F7	Best	4,26E + 01	9,43E − 03	**0,00E + 00**	7,63E − 05	**0,00E + 00**	4,30E − 02	1,30E + 02	**0,00E + 00**	3,90E − 50	7,01E − 197	**0,00E + 00**
	Mean	4,26E + 01	1,65E − 02	**0,00E + 00**	7,63E − 05	**0,00E + 00**	4,31E − 01	1,20E + 02	1,22E − 306	1,04E − 32	1,37E − 73	4,98E − 04
	Std	7,67E − 15	1,80E − 02	**0,00E + 00**	0,00E + 00	**0,00E + 00**	4,72E − 01	1,31E + 01	0,00E + 00	2,74E − 32	3,63E − 73	1,32E − 03
	Ave-Time (s)	2,44E − 03	6,30E − 03	6,63E − 04	6,41E − 03	1,66E − 02	3,34E − 03	1,25E − 03	1,14E − 03	7,23E − 04	3,18E − 03	5,77E − 04
	Rank	10	8	**1**	6	**1**	9	11	3	5	4	7
F8	Best	1,21E + 09	2,50E + 05	3,49E − 05	9,90E + 01	4,06E − 09	5,05E + 05	1,72E + 04	1,23E − 02	9,60E + 01	**0,00E + 00**	9,90E + 01
	Mean	1,26E + 09	2,64E + 05	1,18E − 02	9,90E + 01	5,01E − 09	6,33E + 06	9,76E + 05	8,83E − 02	9,61E + 01	**3,02E − 14**	2,38E + 03
	Std	7,32E + 07	3,45E + 04	2,15E − 02	1,53E − 14	6,45E − 10	6,53E + 06	2,24E + 06	9,19E − 02	7,30E − 02	7,99E − 14	6,02E + 03
	Ave-Time (s)	1,46E − 03	3,02E − 03	3,66E − 04	3,75E − 03	9,39E − 03	2,15E − 03	3,96E − 04	6,03E − 04	3,80E − 04	1,88E − 03	2,90E − 04
	Rank	10	8	3	6	2	11	9	4	5	**1**	7

Table 3: Continued.

Function	Criterion	ABC	ASO	AVOA	ESO	ESSA	FFA	GA	GTO	GWO	MGO	PSO
F9	Best	1,93E + 13	3,59E + 07	**0,00E + 00**	1,80E − 05	**0,00E + 00**	6,62E + 10	7,23E + 12	**0,00E + 00**	1,58E + 04	1,48E − 101	6,09E + 09
	Mean	2,05E + 13	3,59E + 07	7,26E − 248	1,80E − 05	**0,00E + 00**	9,78E + 10	9,30E + 12	3,76E − 154	3,14E + 06	5,64E − 33	2,30E + 10
	Std	2,02E + 12	7,43E + 04	0,00E + 00	3,66E − 21	**0,00E + 00**	2,55E + 10	1,59E + 12	9,94E − 154	4,00E + 06	1,49E − 32	1,65E + 10
	Ave-Time (s)	1,90E − 03	7,16E − 03	4,90E − 04	4,82E − 03	1,16E − 02	2,61E − 03	7,98E − 04	8,36E − 04	5,50E − 04	2,44E − 03	4,47E − 04
	Rank	11	7	2	5	**1**	9	10	3	6	4	8
F10	Best	6,84E + 10	1,13E + 06	**0,00E + 00**	3,27E − 10	**0,00E + 00**	2,35E + 03	2,04E + 09	**0,00E + 00**	9,50E − 51	6,79E − 235	1,00E + 08
	Mean	6,84E + 10	1,15E + 06	**0,00E + 00**	3,27E − 10	**0,00E + 00**	3,10E + 06	9,64E + 09	**0,00E + 00**	1,46E − 32	2,74E − 75	1,00E + 08
	Std	1,65E − 05	4,60E + 04	**0,00E + 00**	0,00E + 00	**0,00E + 00**	6,50E + 06	7,12E + 09	**0,00E + 00**	3,87E − 32	7,25E − 75	0,00E + 00
	Ave-Time (s)	1,41E − 03	6,24E − 03	3,42E − 04	3,63E − 03	9,41E − 03	2,09E − 03	3,90E − 04	5,62E − 04	4,36E − 04	1,96E − 03	2,73E − 04
	Rank	11	7	**1**	6	**1**	8	10	**1**	5	4	9
F11	Best	2,09E + 01	7,62E + 00	**8,88E − 16**	6,65E − 03	**8,88E − 16**	3,59E + 00	5,44E + 00	**8,88E − 16**	3,14E − 13	**8,88E − 16**	9,64E + 00
	Mean	2,09E + 01	7,64E + 00	**8,88E − 16**	6,65E − 03	**8,88E − 16**	6,41E + 00	1,41E + 01	**8,88E − 16**	5,82E − 10	**8,88E − 16**	1,01E + 01
	Std	6,18E − 02	4,63E − 02	**0,00E + 00**	0,00E + 00	**0,00E + 00**	2,54E + 00	5,38E + 00	**0,00E + 00**	1,50E − 09	**0,00E + 00**	8,73E − 01
	Ave-Time (s)	1,62E − 03	3,57E − 03	4,51E − 04	4,39E − 03	1,05E − 02	2,32E − 03	5,86E − 04	5,89E − 04	4,48E − 04	2,04E − 03	3,43E − 04
	Rank	11	8	**1**	6	**1**	7	10	**1**	5	**1**	9
F12	Best	2,42E + 03	3,53E + 00	**0,00E + 00**	4,76E − 01	**0,00E + 00**	1,38E + 00	1,72E + 03	**0,00E + 00**	**0,00E + 00**	**0,00E + 00**	**0,00E + 00**
	Mean	2,43E + 03	3,54E + 00	**0,00E + 00**	4,76E − 01	**0,00E + 00**	1,27E + 01	1,84E + 03	**0,00E + 00**	**0,00E + 00**	**0,00E + 00**	**0,00E + 00**
	Std	4,76E + 00	8,56E − 03	**0,00E + 00**	6,00E − 17	**0,00E + 00**	1,55E + 01	8,69E + 01	**0,00E + 00**	**0,00E + 00**	**0,00E + 00**	**0,00E + 00**
	Ave-Time (s)	1,82E − 03	4,55E − 03	5,18E − 04	4,78E − 03	1,21E − 03	2,45E − 03	7,31E − 04	6,77E − 04	4,18E − 04	2,27E − 03	3,80E − 04
	Rank	11	8	**1**	7	**1**	9	10	**1**	**1**	**1**	**1**
F13	Best	**0,00E + 00**	4,08E − 85	**0,00E + 00**	3,08E − 06	**0,00E + 00**	0,00E + 00	4,69E − 04	**0,00E + 00**	**0,00E + 00**	**0,00E + 00**	**0,00E + 00**
	Mean	3,24E − 99	3,98E − 19	**0,00E + 00**	3,08E − 06	**0,00E + 00**	1,77E − 94	2,17E − 04	1,89E − 130	**0,00E + 00**	**0,00E + 00**	**0,00E + 00**
	Std	8,58E − 99	1,05E − 18	**0,00E + 00**	9,15E − 22	**0,00E + 00**	4,68E − 94	1,82E − 04	5,00E − 130	**0,00E + 00**	**0,00E + 00**	**0,00E + 00**
	Ave-Time (s)	1,77E − 03	3,43E − 03	3,63E − 04	4,13E − 03	1,02E − 02	2,46E − 03	4,95E − 04	6,61E − 04	4,02E − 04	2,28E − 03	3,38E − 04
	Rank	7	9	**1**	10	**1**	8	11	6	**1**	**1**	**1**
F14	Best	1,60E + 03	2,32E + 02	**0,00E + 00**	1,01E − 09	**0,00E + 00**	4,64E + 02	1,08E + 03	**0,00E + 00**	1,14E − 13	**0,00E + 00**	2,41E + 02
	Mean	1,63E + 03	2,38E + 02	**0,00E + 00**	1,01E − 09	**0,00E + 00**	6,24E + 02	1,07E + 03	**0,00E + 00**	1,30E − 13	**0,00E + 00**	2,77E + 02
	Std	5,45E + 01	1,52E + 01	**0,00E + 00**	0,00E + 00	**0,00E + 00**	1,48E + 02	5,37E + 01	**0,00E + 00**	4,30E − 14	**0,00E + 00**	4,41E + 01
	Ave-Time (s)	1,60E − 03	3,43E − 03	3,51E − 04	4,11E − 03	1,05E − 02	2,29E − 03	5,73E − 04	6,17E − 04	4,25E − 04	2,54E − 03	3,34E − 04
	Rank	11	7	**1**	6	**1**	9	10	**1**	5	**1**	8
F15	Best	2,32E + 02	1,64E + 01	**0,00E + 00**	1,44E + 01	**0,00E + 00**	6,72E + 01	1,09E + 02	**0,00E + 00**	9,27E − 16	2,44E − 69	2,73E + 01
	Mean	2,32E + 02	1,69E + 01	6,55E − 153	1,44E + 01	**5,28E − 275**	7,92E + 01	1,30E + 02	1,13E − 79	2,82E − 11	1,02E − 24	2,97E + 01
	Std	0,00E + 00	1,31E + 00	1,73E − 152	0,00E + 00	0,00E + 00	1,13E + 01	1,08E + 01	2,99E − 79	7,36E − 11	2,69E − 24	1,36E + 00
	Ave-Time (s)	1,57E − 03	5,11E − 03	4,21E − 04	4,08E − 03	9,65E − 03	2,31E − 03	5,17E − 04	6,22E − 04	4,11E − 04	2,43E − 03	3,31E − 04
	Rank	11	8	2	7	**1**	10	6	3	5	4	9
Unimodal rank-count (F1–F10)		108	76	20	55	11	90	96	31	53	37	74
Multimodal rank-count (F11–F15)		51	40	6	36	5	43	47	12	17	8	28
Total rank-count		159	116	26	91	16	133	143	43	70	45	102

Table 3: Continued.

Function	Criterion	ABC	ASO	AVOA	ESO	ESSA	FFA	GA	GTO	GWO	MGO	PSO
Unimodal	Ave-rank	10.8	7.6	2	5.5	1.1	9	9.6	3.1	5.3	3.7	7.4
Multimodal	Ave-rank	10.2	8	1.2	7.2	1	8.6	9.4	2.4	1.4	9.2	5.6
Total	Ave-rank	10.6	7.73	1.73	6.06	1.06	8.86	9.53	2.86	4.66	3	6.8
Unimodal	overall rank	11	8	2	6	**1**	9	10	3	5	4	7
Multimodal	overall rank	11	7	2	6	**1**	8	10	4	3	9	5
Total	rverall rank	11	8	2	6	**1**	9	10	3	5	4	7

ESSA, electro search simulated annealing. Bold values indicate the best values in the category.

Table 4: Results of unimodal (F1–F10) and multimodal (F11–F15) functions with 500 dimensions.

Function	Criterion	ABC	ASO	AVOA	ESO	ESSA	FFA	GA	GTO	GWO	MGO	PSO
F1	Best	1,52E + 06	5,08E + 04	**0,00E + 00**	2,10E − 11	**0,00E + 00**	3,85E + 05	8,74E + 05	**0,00E + 00**	6,90E − 11	8,26E − 113	2,99E + 04
	Mean	1,52E + 06	5,08E + 04	3,95E − 278	2,10E − 11	**0,00E + 00**	4,78E + 05	1,04E + 06	8,34E − 160	4,35E − 06	2,19E − 37	4,94E + 04
	Std	2,51E − 10	6,20E + 01	0,00E + 00	3,49E − 27	**0,00E + 00**	7,23E + 04	1,23E + 05	2,21E − 159	1,14E − 05	5,78E − 37	1,42E + 04
	Ave-Time (s)	2,37E − 03	7,30E − 03	1,62E − 03	8,64E − 03	2,13E − 02	3,89E − 03	2,49E − 03	1,96E − 03	1,43E − 03	5,66E − 03	1,23E − 03
	Rank	11	8	2	5	**1**	9	10	3	6	4	7
F2	Best	4,83E + 03	1,19E + 03	7,74E − 268	1,15E − 06	**0,00E + 00**	1,96E + 03	1,69E + 03	**0,00E + 00**	8,23E − 07	7,99E − 63	1,24E + 03
	Mean	4,83E + 03	1,19E + 03	1,49E − 130	1,15E − 06	**1,97E − 269**	2,14E + 03	1,87E + 03	7,50E − 82	1,12E − 04	5,61E − 22	1,26E + 03
	Std	9,82E − 13	6,21E + 00	3,93E − 130	0,00E + 00	**0,00E + 00**	1,72E + 02	1,95E + 02	1,98E − 81	2,65E − 04	1,49E − 21	1,77E + 01
	Ave-Time (s)	1,91E − 03	6,06E − 03	1,31E − 03	8,14E − 03	2,14E − 02	2,95E − 03	1,61E − 03	1,73E − 03	1,45E − 03	5,16E − 03	7,13E − 04
	Rank	11	7	2	5	**1**	10	9	3	6	4	8
F3	Best	3,29E + 07	1,04E + 06	**0,00E + 00**	5,06E + 06	6,47E − 63	4,43E + 06	2,82E + 06	**0,00E + 00**	1,08E + 05	2,54E + 02	2,53E + 06
	Mean	3,29E + 07	1,04E + 06	**1,33E − 190**	5,06E + 06	6,47E − 63	4,86E + 06	4,37E + 06	2,54E − 133	3,38E + 05	1,29E + 03	2,60E + 06
	Std	8,05E − 09	2,65E + 03	0,00E + 00	0,00E + 00	0,00E + 00	4,08E + 05	1,34E + 06	6,72E − 133	2,58E + 05	1,21E + 03	4,92E + 04
	Ave-Time (s)	4,64E − 02	3,11E − 02	1,65E − 02	1,33E − 01	3,98E − 01	4,73E − 02	4,00E − 02	2,66E − 02	1,43E − 02	6,05E − 02	1,28E − 02
	Rank	11	6	**1**	10	3	9	8	2	5	4	7
F4	Best	9,92E + 01	5,84E + 01	2,75E − 256	1,79E + 00	**0,00E + 00**	9,92E + 01	8,41E + 01	**0,00E + 00**	5,72E + 01	1,79E − 36	1,41E + 01
	Mean	9,92E + 01	5,84E + 01	3,95E − 124	1,79E + 00	**1,22E − 258**	9,92E + 01	8,69E + 01	6,81E − 84	7,91E + 01	1,83E − 15	2,87E + 01
	Std	1,53E − 14	4,39E − 02	1,05E − 123	2,40E − 16	0,00E + 00	1,53E − 14	1,92E + 00	1,80E − 83	1,62E + 01	4,83E − 15	1,75E + 01
	Ave-Time (s)	1,82E − 03	6,64E − 03	1,26E − 03	8,06E − 03	9,41E − 03	3,03E − 03	1,71E − 03	1,71E − 03	1,37E − 03	5,24E − 03	5,20E − 04
	Rank	10	7	2	5	1	10	8	3	9	4	6
F5	Best	4,03E + 06	3,38E + 05	**0,00E + 00**	7,61E + 02	**0,00E + 00**	8,17E + 05	3,69E + 05	**0,00E + 00**	8,35E − 11	7,23E − 112	6,14E + 04
	Mean	4,03E + 06	3,39E + 05	2,42E − 300	7,61E + 02	**0,00E + 00**	9,85E + 05	4,91E + 05	1,39E − 152	4,03E − 06	2,63E − 37	6,89E + 04
	Std	5,03E − 10	2,60E + 03	0,00E + 00	1,23E − 13	**0,00E + 00**	1,47E + 05	1,63E + 05	3,69E − 152	1,05E − 05	6,96E − 37	1,05E + 04
	Ave-Time (s)	1,81E − 03	8,47E − 03	1,28E − 03	8,05E − 03	1,64E − 02	2,87E − 03	1,52E − 03	1,74E − 03	1,35E − 03	5,27E − 03	5,19E − 04
	Rank	11	8	2	6	**1**	10	9	3	5	4	7
F6	Best	1,54E + 06	5,57E + 04	5,31E − 03	7,84E + 01	1,47E − 05	4,36E + 05	8,89E + 05	8,62E − 01	9,58E + 01	1,08E − 04	8,97E + 04
	Mean	1,54E + 06	5,57E + 04	1,42E − 02	7,84E + 01	1,03E − 01	4,94E + 05	1,05E + 06	1,82E + 00	9,91E + 01	**1,85E − 04**	9,61E + 04
	Std	0,00E + 00	8,92E + 01	1,13E − 02	0,00E + 00	2,70E − 01	4,52E + 04	1,23E + 05	7,98E − 01	3,09E + 00	5,46E − 05	9,32E + 03
	Ave-Time (s)	1,87E − 03	8,09E − 03	1,24E − 03	8,05E − 03	1,03E − 02	2,82E − 03	1,50E − 03	1,67E − 03	1,37E − 03	5,21E − 03	4,99E − 04
	Rank	11	8	2	6	3	10	5	4	7	**1**	9
F7	Best	2,47E + 02	5,62E + 00	**0,00E + 00**	8,38E − 08	**0,00E + 00**	6,10E + 01	1,72E + 04	**0,00E + 00**	6,75E − 24	3,54E − 206	4,15E − 03
	Mean	2,47E + 02	5,80E + 00	**0,00E + 00**	8,38E − 08	**0,00E + 00**	6,85E + 01	1,71E + 04	3,28E − 288	1,00E − 13	5,68E − 74	1,11E − 01
	Std	0,00E + 00	4,03E − 01	**0,00E + 00**	0,00E + 00	**0,00E + 00**	7,24E + 00	1,09E + 03	0,00E + 00	2,66E − 13	1,50E − 73	1,78E − 01
	Ave-Time (s)	6,73E − 03	1,02E − 02	2,73E − 03	2,24E − 02	2,29E − 02	7,77E − 03	8,24E − 03	4,38E − 03	2,88E − 03	1,17E − 02	2,08E − 03
	Rank	10	8	**1**	5	**1**	9	11	3	4	4	7
F8	Best	6,81E + 09	5,37E + 07	8,54E − 05	4,97E + 02	4,76E − 08	1,36E + 09	1,29E + 08	5,26E + 00	4,98E + 02	**0,00E + 00**	8,12E + 07
	Mean	6,81E + 09	5,40E + 07	4,16E − 01	4,97E + 02	3,13E − 07	1,93E + 09	6,99E + 08	1,10E + 01	4,98E + 02	**5,82E − 12**	8,20E + 07
	Std	0,00E + 00	6,40E + 05	3,86E − 01	6,14E − 14	4,53E − 07	4,73E + 08	5,87E + 08	4,32E + 00	1,46E − 01	1,54E − 11	1,30E + 06
	Ave-Time (s)	1,86E − 03	7,58E − 03	1,30E − 03	8,69E − 03	1,80E − 02	3,56E − 03	2,05E − 03	1,77E − 03	1,39E − 03	5,68E − 03	5,28E − 04
	Rank	11	7	3	5	2	10	9	4	6	**1**	8

Table 4: Continued.

Function	Criterion	ABC	ASO	AVOA	ESO	ESSA	FFA	GA	GTO	GWO	MGO	PSO
F9	Best	2,09E + 14	1,17E + 10	**0,00E + 00**	4,93E + 12	**0,00E + 00**	1,60E + 13	1,36E + 14	**0,00E + 00**	1,46E + 00	6,04E − 108	4,68E + 11
	Mean	2,09E + 14	1,17E + 10	1,15E − 247	4,93E + 12	**0,00E + 00**	1,98E + 13	1,48E + 14	2,53E − 136	5,51E + 05	1,99E − 37	8,65E + 11
	Std	3,38E − 02	2,19E + 07	0,00E + 00	0,00E + 00	**0,00E + 00**	3,98E + 12	9,41E + 12	6,70E − 136	1,37E + 06	5,27E − 37	4,40E + 11
	Ave-Time (s)	4,30E − 03	8,64E − 03	2,05E − 03	1,38E − 02	3,60E − 02	5,58E − 03	5,08E − 03	3,08E − 03	2,12E − 03	8,21E − 03	1,31E − 03
	Rank	11	6	2	8	**1**	9	10	3	5	4	7
F10	Best	2,34E + 12	3,04E + 09	**0,00E + 00**	1,60E − 20	**0,00E + 00**	1,39E + 11	6,72E + 11	**0,00E + 00**	5,90E − 22	8,60E − 234	5,21E + 09
	Mean	2,34E + 12	3,04E + 09	**0,00E + 00**	1,60E − 20	**0,00E + 00**	1,91E + 11	9,74E + 11	1,27E − 296	2,22E − 11	2,94E − 69	6,25E + 09
	Std	0,00E + 00	8,42E + 06	**0,00E + 00**	3,25E − 36	**0,00E + 00**	4,84E + 10	2,35E + 11	**0,00E + 00**	5,88E − 11	7,79E − 69	1,11E + 09
	Ave-Time (s)	1,92E − 03	7,03E − 03	1,24E − 03	8,58E − 03	1,96E − 02	2,85E − 03	1,58E − 03	1,71E − 03	1,40E − 03	5,22E − 03	5,36E − 04
	Rank	11	7	**1**	5	**1**	9	10	**3**	6	4	8
F11	Best	2,12E + 01	1,35E + 01	**8,88E − 16**	1,89E − 05	**8,88E − 16**	1,90E + 01	2,06E + 01	**8,88E − 16**	2,12E − 07	**8,88E − 16**	1,26E + 01
	Mean	2,12E + 01	1,35E + 01	**8,88E − 16**	1,89E − 05	**8,88E − 16**	1,94E + 01	2,08E + 01	**8,88E − 16**	2,70E − 05	**8,88E − 16**	1,37E + 01
	Std	0,00E + 00	2,17E − 02	**0,00E + 00**	0,00E + 00	**0,00E + 00**	2,66E − 01	1,15E − 01	**0,00E + 00**	6,33E − 05	**0,00E + 00**	9,70E − 01
	Ave-Time (s)	2,83E − 03	7,72E − 03	1,32E − 03	1,02E − 02	1,52E − 02	3,91E − 03	3,22E − 03	1,75E − 03	1,56E − 03	5,87E − 03	7,95E − 04
	Rank	11	7	**1**	5	**1**	9	10	**1**	6	**1**	8
F12	Best	1,38E + 04	1,03E + 02	**0,00E + 00**	1,69E − 03	**0,00E + 00**	3,42E + 03	1,19E + 04	**0,00E + 00**	6,75E − 12	**0,00E + 00**	6,38E + 01
	Mean	1,38E + 04	1,03E + 02	**0,00E + 00**	1,69E − 03	**0,00E + 00**	3,94E + 03	1,22E + 04	**0,00E + 00**	4,23E − 07	**0,00E + 00**	1,51E + 02
	Std	0,00E + 00	5,68E − 02	**0,00E + 00**	0,00E + 00	**0,00E + 00**	4,13E + 02	2,16E + 02	**0,00E + 00**	1,11E − 06	**0,00E + 00**	7,97E + 01
	Ave-Time (s)	3,75E − 03	8,18E − 03	1,66E − 03	1,34E − 02	1,96E − 02	5,16E − 03	3,95E − 03	2,25E − 03	1,83E − 03	6,81E − 03	1,13E − 03
	Rank	11	7	**1**	6	**1**	9	10	**1**	**5**	**1**	**8**
F13	Best	**0,00E + 00**	1,77E − 93	**0,00E + 00**	7,30E − 04	**0,00E + 00**	**0,00E + 00**	**1,00E + 00**	**0,00E + 00**	**0,00E + 00**	**0,00E + 00**	**0,00E + 00**
	Mean	9,40E − 101	1,19E − 25	**0,00E + 00**	7,30E − 04	**0,00E + 00**	1,86E − 97	1,10E + 00	7,11E − 134	**0,00E + 00**	**0,00E + 00**	**0,00E + 00**
	Std	2,49E − 100	3,16E − 25	**0,00E + 00**	1,17E − 19	**0,00E + 00**	4,93E − 97	5,78E − 02	1,88E − 133	**0,00E + 00**	**0,00E + 00**	**0,00E + 00**
	Ave-Time (s)	2,73E − 03	8,05E − 03	1,54E − 03	1,03E − 02	1,57E − 02	3,58E − 03	2,71E − 03	2,04E − 03	1,61E − 03	6,20E − 03	9,52E − 04
	Rank	7	9	**1**	10	**1**	8	11	6	**1**	**1**	**1**
F14	Best	8,87E + 03	3,20E + 03	**0,00E + 00**	2,05E + 01	**0,00E + 00**	6,58E + 03	8,76E + 03	**0,00E + 00**	6,44E + 00	**0,00E + 00**	1,41E + 03
	Mean	8,87E + 03	3,23E + 03	**0,00E + 00**	2,05E + 01	**0,00E + 00**	6,63E + 03	8,68E + 03	**0,00E + 00**	1,19E + 01	**0,00E + 00**	1,81E + 03
	Std	0,00E + 00	6,65E + 01	**0,00E + 00**	0,00E + 00	**0,00E + 00**	7,66E + 01	1,07E + 02	**0,00E + 00**	6,86E + 00	**0,00E + 00**	5,72E + 02
	Ave-Time (s)	2,81E − 03	8,23E − 03	1,37E − 03	1,05E − 02	1,80E − 02	3,87E − 03	3,25E − 03	1,88E − 03	1,50E − 03	5,98E − 03	8,17E − 04
	Rank	11	8	**1**	6	**1**	9	10	**1**	5	**1**	7
F15	Best	1,39E + 03	3,49E + 02	8,65E − 294	2,97E − 01	**0,00E + 00**	7,51E + 02	1,14E + 03	**0,00E + 00**	4,20E − 03	4,29E − 56	2,51E + 02
	Mean	1,39E + 03	3,51E + 02	1,14E − 149	2,97E − 01	**8,54E − 274**	8,82E + 02	1,11E + 03	5,58E − 80	6,07E − 03	1,71E − 15	2,68E + 02
	Std	2,46E − 13	2,95E + 00	3,03E − 149	6,00E − 17	0,00E + 00	7,95E + 01	2,15E + 01	1,48E − 79	2,42E − 03	4,53E − 15	1,84E + 01
	Ave-Time (s)	2,72E − 03	7,90E − 03	1,37E − 03	1,04E − 02	3,51E − 02	3,73E − 03	3,03E − 03	1,96E − 03	1,52E − 03	5,72E − 03	7,41E − 04
	Rank	11	7	2	6	**1**	9	10	3	5	4	8
Unimodal rank-count (F1–F10)		108	72	18	65	13	85	80	31	58	34	74
Multimodal rank-count (F11–F15)		51	38	6	33	5	44	51	12	23	8	32
Total rank-count		159	110	24	98	18	129	131	43	81	42	106

Table 4: Continued.

Function	Criterion	ABC	ASO	AVOA	ESO	ESSA	FFA	GA	GTO	GWO	MGO	PSO
Unimodal	Ave-rank	10.8	7.2	1.8	6.5	1.3	8.5	8	3.1	5.8	3.4	7.4
Multimodal	Ave-rank	10.2	7.6	1.2	6.6	1	8.8	10.2	2.4	4.6	1.6	6.4
Total	Ave-rank	10.6	7.3	1.6	6.53	1.2	8.6	8.7	2.86	5.4	2.8	7.06
Unimodal	overall- rank	11	7	2	6	**1**	10	9	3	5	4	8
Multimodal	overall rank	10	8	2	7	**1**	9	10	4	5	3	6
Total	overall rank	11	8	2	6	**1**	9	10	4	5	3	7

ESSA, electro search simulated annealing. Bold values indicate the best values in the category.

Table 5: Results of unimodal (F1–F10) and multimodal (F11–F15) functions with 1,000 dimensions.

Function	Criterion	ABC	ASO	AVOA	ESO	ESSA	FFA	GA	GTO	GWO	MGO	PSO
F1	Best	2,77E + 06	8,58E + 04	**0,00E + 00**	1,64E−03	**0,00E + 00**	1,07E + 06	1,90E + 06	**0,00E + 00**	4,19E−08	7,58E−103	4,95E + 05
	Mean	2,77E + 06	8,58E + 04	1,13E−252	1,64E−03	**0,00E + 00**	1,18E + 06	2,14E + 06	5,05E−151	3,08E−04	5,98E−30	4,98E + 05
	Std	5,03E−10	4,29E + 01	0,00E + 00	0,00E + 00	**0,00E + 00**	8,80E + 04	1,78E + 05	1,34E−150	7,95E−04	1,58E−29	5,78E + 03
	Ave-Time (s)	3,19E−03	1,26E−02	2,14E−03	1,38E−02	2,24E−02	4,84E−03	3,11E−03	2,89E−03	2,84E−03	8,90E−03	1,21E−03
	Rank	11	7	2	6	**1**	9	10	3	5	4	8
F2	Best	8,77E + 03	2,29E + 03	8,69E−300	1,03E−08	**0,00E + 00**	4,53E + 03	4,31E + 03	**0,00E + 00**	6,13E−05	2,85E−63	1,03E + 03
	Mean	8,77E + 03	2,29E + 03	1,58E−156	1,03E−08	**2,13E−261**	4,70E + 03	4,71E + 03	3,49E−76	3,50E−03	1,75E−19	1,05E + 03
	Std	0,00E + 00	6,11E + 00	4,19E−156	0,00E + 00	**0,00E + 00**	1,60E + 02	4,31E + 02	9,25E−76	7,83E−03	4,62E−19	3,14E + 01
	Ave-time (s)	2,26E−03	1,27E−02	1,39E−03	1,34E−02	2,08E−02	3,62E−03	3,20E−03	2,23E−03	2,47E−03	8,11E−03	6,90E−04
	Rank	11	8	2	5	**1**	9	10	3	6	4	7
F3	Best	1,61E + 08	9,11E + 06	**0,00E + 00**	3,15E + 00	**0,00E + 00**	1,67E + 07	1,11E + 07	**0,00E + 00**	8,27E + 05	5,20E + 03	2,06E + 07
	Mean	1,61E + 08	9,11E + 06	1,01E−182	3,15E + 00	**0,00E + 00**	1,75E + 07	1,75E + 07	1,60E−122	1,82E + 06	1,21E + 04	2,27E + 07
	Std	1,56E + 06	5,65E + 02	0,00E + 00	0,00E + 00	**0,00E + 00**	5,11E + 05	5,37E + 06	4,23E−122	1,00E + 06	7,51E + 03	1,56E + 06
	Ave-time (s)	1,00E−01	7,18E−02	3,20E−02	2,87E−01	7,92E−01	9,82E−02	8,41E−02	6,86E−02	3,00E−02	1,25E−01	2,77E−02
	Rank	11	7	**2**	4	**1**	8	9	3	6	5	10
F4	Best	9,95E + 01	6,05E + 01	3,54E−277	1,92E + 01	**0,00E + 00**	9,95E + 01	9,10E + 01	**0,00E + 00**	7,63E + 01	2,35E−37	3,88E + 01
	Mean	9,95E + 01	6,05E + 01	4,69E−131	1,92E + 01	**1,45E−258**	9,95E + 01	9,25E + 01	4,64E−82	9,18E + 01	3,08E−14	4,07E + 01
	Std	0,00E + 00	6,13E−03	1,24E−130	3,84E−15	**0,00E + 00**	0,00E + 00	1,25E + 00	1,23E−81	9,13E + 00	8,14E−14	2,15E + 00
	Ave-time (s)	3,23E−03	9,63E−03	1,34E−03	1,23E−02	1,33E−02	3,45E−03	3,24E−03	2,49E−03	3,01E−03	7,84E−03	6,47E−04
	Rank	10	7	2	5	**1**	10	9	3	8	4	6
F5	Best	1,26E + 07	1,18E + 06	**0,00E + 00**	6,22E−12	**0,00E + 00**	4,28E + 06	2,37E + 06	**0,00E + 00**	1,89E−07	1,09E−109	1,41E + 05
	Mean	1,26E + 07	1,18E + 06	1,79E−292	6,22E−12	**0,00E + 00**	4,68E + 06	3,37E + 06	8,63E−149	2,88E−03	4,12E−35	2,72E + 05
	Std	2,01E−09	7,21E + 03	0,00E + 00	8,73E−28	**0,00E + 00**	2,84E + 05	9,68E + 05	2,28E−148	7,48E−03	1,09E−34	1,63E + 05
	Ave-time (s)	2,19E−03	1,13E−02	1,46E−03	1,33E−02	2,38E−02	3,51E−03	3,20E−03	2,87E−03	2,48E−03	8,06E−03	6,80E−04
	Rank	11	8	2	5	**1**	10	9	3	6	4	7
F6	Best	2,80E + 06	7,75E + 04	1,08E−01	2,24E + 02	2,43E−05	1,08E + 06	1,92E + 06	6,32E−01	1,89E + 02	7,89E−03	1,29E + 05
	Mean	2,80E + 06	7,75E + 04	1,27E−01	2,24E + 02	**1,30E−04**	1,20E + 06	2,16E + 06	9,05E−01	1,94E + 02	1,01E−02	1,46E + 05
	Std	5,03E−10	6,41E + 01	1,77E−02	3,07E−14	6,63E−05	9,88E + 04	1,80E + 05	2,02E−01	4,69E + 00	1,77E−03	1,72E + 04
	Ave-time (s)	2,26E−03	9,83E−03	1,39E−03	1,26E−02	1,68E−02	3,37E−03	3,29E−03	2,43E−03	2,42E−03	7,94E−03	6,94E−04
	Rank	10	6	3	9	**1**	8	11	4	5	**2**	7
F7	Best	4,38E + 02	1,63E + 01	**0,00E + 00**	1,64E−11	**0,00E + 00**	2,18E + 02	9,96E + 04	0,00E + 00	7,06E−20	3,24E−184	3,63E + 00
	Mean	4,38E + 02	1,66E + 01	**0,00E + 00**	1,64E−11	**0,00E + 00**	2,48E + 02	8,29E + 04	2,38E−307	3,06E−11	2,80E−65	5,81E + 00
	Std	0,00E + 00	6,43E−01	**0,00E + 00**	0,00E + 00	**0,00E + 00**	3,05E + 01	1,25E + 04	0,00E + 00	8,08E−11	7,40E−65	1,94E + 00
	Ave-time (s)	1,13E−02	1,63E−02	5,18E−03	3,61E−02	6,08E−02	1,24E−02	1,18E−02	8,42E−03	5,21E−03	1,95E−02	3,70E−03
	Rank	10	8	**1**	5	**1**	9	11	3	6	4	7
F8	Best	1,29E + 10	8,42E + 07	1,78E−02	9,51E + 02	1,31E−04	5,00E + 09	1,19E + 09	1,40E + 00	8,97E + 02	6,12E−28	2,48E + 08
	Mean	1,29E + 10	8,43E + 07	1,04E + 00	9,51E + 02	3,49E−04	6,69E + 09	2,95E + 09	2,16E + 00	8,98E + 02	**4,78E−12**	2,55E + 08
	Std	0,00E + 00	3,01E + 05	6,02E−01	0,00E + 00	5,71E−04	1,07E + 09	1,58E + 09	5,31E−01	1,27E + 00	1,27E−11	8,49E + 06
	Ave-time (s)	2,41E−03	1,11E−02	1,85E−03	1,41E−02	2,44E−02	3,60E−03	3,42E−03	2,46E−03	2,50E−03	8,40E−03	8,11E−04
	Rank	11	7	3	6	2	10	9	4	5	**1**	8

Table 5: Continued.

Function	Criterion	ABC	ASO	AVOA	ESO	ESSA	FFA	GA	GTO	GWO	MGO	PSO
	Best	3,98E + 14	1,98E + 10	**0,00E + 00**	1,63E + 13	**0,00E + 00**	7,52E + 13	2,83E + 14	**0,00E + 00**	1,87E + 04	7,58E−114	6,32E + 12
	Mean	3,98E + 14	1,98E + 10	5,04E−227	1,63E + 13	**0,00E + 00**	8,32E + 13	3,02E + 14	1,08E−148	1,48E + 07	2,95E−36	9,24E + 12
F9	Std	0,00E + 00	6,15E + 07	0,00E + 00	4,22E−03	**0,00E + 00**	9,01E + 12	1,41E + 13	2,85E−148	3,25E + 07	7,81E−36	2,67E + 12
	Ave-time (s)	6,70E−03	1,28E−02	5,54E−03	2,28E−02	4,41E−02	7,95E−03	8,15E−03	5,22E−03	3,79E−03	1,35E−02	2,24E−03
	Rank	11	6	2	8	**1**	9	10	3	5	4	7
	Best	8,26E + 12	9,12E + 09	**0,00E + 00**	9,31E−19	**0,00E + 00**	1,24E + 12	3,74E + 12	**0,00E + 00**	2,57E−15	5,93E−223	1,36E + 10
	Mean	8,26E + 12	9,12E + 09	**0,00E + 00**	9,31E−19	**0,00E + 00**	1,44E + 12	4,76E + 12	**0,00E + 00**	2,92E−06	1,77E−77	1,46E + 10
F10	Std	0,00E + 00	1,48E + 07	**0,00E + 00**	0,00E + 00	**0,00E + 00**	1,55E + 11	7,68E + 11	**0,00E + 00**	7,73E−06	4,68E−77	9,49E + 08
	Ave-time (s)	2,26E−03	1,05E−02	1,93E−03	1,33E−02	1,99E−02	3,48E−03	3,18E−03	2,24E−03	2,45E−03	8,02E−03	9,62E−04
	Rank	11	7	**1**	5	**1**	9	10	**1**	6	4	8
	Best	2,12E + 01	1,45E + 01	**8,88E−16**	3,46E−07	**8,88E−16**	2,00E + 01	2,10E + 01	**8,88E−16**	1,02E−05	8,88E−16	1,26E + 01
	Mean	2,12E + 01	1,45E + 01	**8,88E−16**	3,46E−07	**8,88E−16**	2,02E + 01	2,10E + 01	**8,88E−16**	4,57E−04	1,90E−15	1,32E + 01
F11	Std	0,00E + 00	1,11E−02	**0,00E + 00**	0,00E + 00	**0,00E + 00**	1,38E−01	3,96E−02	**0,00E + 00**	9,93E−04	1,73E−15	6,83E−01
	Ave-time (s)	4,33E−03	1,15E−02	1,96E−03	1,62E−02	3,27E−02	5,41E−03	5,07E−03	2,76E−03	2,62E−03	9,17E−03	1,88E−03
	Rank	11	8	**1**	5	**1**	10	9	**1**	6	**4**	7
	Best	2,51E + 04	2,08E + 02	**0,00E + 00**	3,17E + 02	**0,00E + 00**	9,65E + 03	2,31E + 04	**0,00E + 00**	1,81E−09	**0,00E + 00**	1,32E + 03
	Mean	2,51E + 04	2,08E + 02	**0,00E + 00**	3,17E + 02	**0,00E + 00**	1,07E + 04	2,35E + 04	**0,00E + 00**	3,05E−05	**0,00E + 00**	1,79E + 03
F12	Std	3,93E−12	5,75E−02	**0,00E + 00**	0,00E + 00	**0,00E + 00**	7,19E + 02	3,04E + 02	**0,00E + 00**	7,94E−05	**0,00E + 00**	4,32E + 02
	Ave-time (s)	5,70E−03	1,39E−02	2,59E−03	2,20E−02	4,93E−02	7,39E−03	6,68E−03	3,75E−03	3,04E−03	1,09E−02	3,68E−03
	Rank	11	7	**1**	8	**1**	9	10	**1**	5	**1**	6
	Best	2,90E−100	1,35E−93	**0,00E + 00**	1,59E−07	**0,00E + 00**	**0,00E + 00**	3,31E−04	**0,00E + 00**	**0,00E + 00**	**0,00E + 00**	**0,00E + 00**
	Mean	2,90E−100	9,12E−28	**0,00E + 00**	1,59E−07	**0,00E + 00**	1,81E−98	6,63E−04	7,41E−132	**0,00E + 00**	**0,00E + 00**	**0,00E + 00**
F13	Std	7,68E−100	2,41E−27	**0,00E + 00**	0,00E + 00	**0,00E + 00**	4,80E−98	1,03E−03	1,96E−131	**0,00E + 00**	**0,00E + 00**	**0,00E + 00**
	Ave-time (s)	3,45E−03	9,80E−03	2,28E−03	1,60E−02	3,31E−02	5,36E−03	4,79E−03	3,11E−03	2,82E−03	1,09E−02	2,32E−03
	Rank	7	9	**1**	10	**1**	8	11	6	**1**	**1**	**1**
	Best	1,62E + 04	7,05E + 03	**0,00E + 00**	2,86E−05	**0,00E + 00**	1,17E + 04	1,83E + 04	**0,00E + 00**	7,47E + 00	**0,00E + 00**	3,50E + 03
	Mean	1,62E + 04	7,09E + 03	**0,00E + 00**	2,86E−05	**0,00E + 00**	1,21E + 04	1,85E + 04	**0,00E + 00**	1,49E + 01	**0,00E + 00**	3,63E + 03
F14	Std	0,00E + 00	8,49E + 01	**0,00E + 00**	0,00E + 00	**0,00E + 00**	4,23E + 02	2,20E + 02	**0,00E + 00**	1,20E + 01	**0,00E + 00**	2,86E + 02
	Ave-time (s)	4,08E−03	1,05E−02	1,76E−03	1,88E−02	2,51E−02	5,72E−03	4,76E−03	2,86E−03	2,66E−03	9,49E−03	2,78E−03
	Rank	10	38	**1**	5	**1**	9	11	**1**	6	**1**	7
	Best	2,56E + 03	7,51E + 02	1,26E−276	8,51E−06	**0,00E + 00**	1,79E + 03	2,57E + 03	**0,00E + 00**	8,12E−03	1,26E−66	5,88E + 02
	Mean	2,56E + 03	7,53E + 02	3,53E−140	8,51E−06	**3,44E−261**	1,81E + 03	2,47E + 03	1,49E−79	1,22E−02	2,09E−23	5,92E + 02
F15	Std	4,91E−13	4,08E + 00	9,34E−140	0,00E + 00	**0,00E + 00**	2,97E + 01	6,13E + 01	3,95E−79	7,26E−03	5,52E−23	5,60E + 00
	Ave-time (s)	3,82E−03	9,64E−03	1,70E−03	1,79E−02	2,51E−02	5,16E−03	4,77E−03	2,97E−03	2,60E\−03	9,44E−03	2,49E−03
	Rank	11	8	2	5	**1**	9	10	3	6	4	7
Unimodal rank-count (F1–F10)		107	71	20	58	11	91	98	30	58	36	75
Multimodal rank-count (F11–F15)		50	40	6	33	5	45	51	12	24	11	28
Total rank-count		157	141	26	91	16	136	149	42	82	47	103

Table 5: Continued.

Function	Criterion	ABC	ASO	AVOA	ESO	ESSA	FFA	GA	GTO	GWO	MGO	PSO
Unimodal	Ave-rank	10,7	7,1	2	5,8	1,1	9,1	9,8	3	5,8	3,6	7,5
Multimodal	Ave-rank	10	8	1,2	6,6	1	9	10,2	2,4	4,8	2,2	5,6
Total	Ave-rank	10,46	7,4	1,73	6,06	1,06	9,06	9,93	2,8	5,46	3,13	6,86
Unimodal	overall rank	10	6	2	5	**1**	8	9	3	5	4	7
Multimodal	overall rank	10	8	2	7	**1**	9	11	4	5	3	6
Total	overall rank	11	8	2	6	**1**	9	10	3	5	4	7

ESSA, electro search simulated annealing. Bold values indicate the best values in the category.

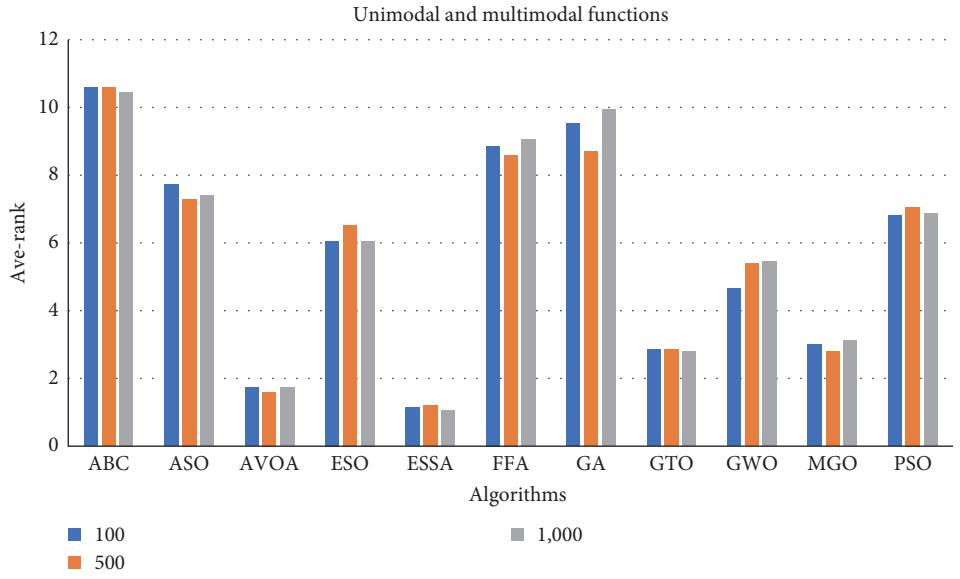

Figure 4: Average rank of functions by Friedman test.

Table 6: Wilcoxon signed-rank test for unimodal functions.

	$N = 100$		$N = 500$		$N = 1{,}000$	
	P	h	P	h	P	h
ESSA vs. ABC	6.2553E−217	1	1.4861E−217	1	9.2058E−218	1
ESSA vs. ASO	3.3089E−165	1	3.1224E−165	1	3.0527E−165	1
ESSA vs. AVOA	1.598E−73	1	1.3309E−76	1	3.8484E−83	1
ESSA vs. ESO	1.4314E−212	1	1.3828E−213	1	8.3096E−214	1
ESSA vs. FFA	3.2960E−165	1	1.2849E−165	1	2.7260E−165	1
ESSA vs. GA	3.3259E−165	1	3.3259E−165	1	3.3359E−165	1
ESSA vs. GTO	9.1319E−103	1	3.256E−103	1	4.6752E−103	1
ESSA vs. GWO	3.3257E−165	1	3.3256E−165	1	5.1466E−164	1
ESSA vs. MGO	4.7508E−160	1	6.6542E−164	1	6.6539E−164	1
ESSA vs. PSO	1.5775E−131	1	2.7426E−165	1	1.7686E−165	1

ESSA, electro search simulated annealing.

Table 7: Wilcoxon signed-rank test for multimodal functions.

	$N = 100$		$N = 500$		$N = 1{,}000$	
	P	h	P	h	P	h
ESSA vs. ABC	3.9932E−189	1	2.6615E−215	1	6.6113E−216	1
ESSA vs. ASO	2.0103E−164	1	3.2634E−165	1	3.2046E−165	1
ESSA vs. AVOA	6.1778E−164	1	3.1057E−165	1	3.2157E−165	1
ESSA vs. ESO	6.6742E−215	1	1.6618E−214	1	5.9527E−213	1
ESSA vs. FFA	2.6130E−165	1	3.3259E−165	1	5.0938E−168	1
ESSA vs. GA	3.3359E\−165	1	3.4255E−165	1	3.3359E−165	1
ESSA vs. GTO	1.5072E−149	1	2.4336E−149	1	4.6495E−149	1
ESSA vs. GWO	5.2086E−164	1	3.3258E−165	1	3.3234E−165	1
ESSA vs. MGO	4.3870E−160	1	4.5712E−165	1	6.6550E−164	1
ESSA vs. PSO	1.9779E−165	1	1.9638E−165	1	1.3583E−165	1

ESSA, electro search simulated annealing.

Table 8: Total execution time.

		Iteration (i)	Ave-time (t) (s)	Total time ($i \times t$) (s)	N
F4	PSO	395	3,39E − 04	1,34E − 01	100
	ESSA	468	6,10E − 03	2,85E + 00	
F7	AVOA	239	6,63E − 04	1,58E − 01	500
	ESSA	118	1,66E − 02	1,96E + 00	
F10	AVOA	255	3,42E − 04	8,72E − 02	1,000
	ESSA	203	9,41E − 03	1,91E + 00	
	GTO	400	5,62E − 04	2,25E − 01	
F12	AVOA	35	5,18E − 04	1,81E − 02	100
	ESSA	25	1,21E − 03	3,03E − 02	
	GWO	394	6,77E − 04	2,67E − 01	
	GTO	82	4,18E − 04	3,43E − 02	
	MGO	65	2,27E − 03	1,48E − 01	
	PSO	258	3,80E − 04	9,80E − 02	
F13	AVOA	291	1,54E − 03	4,48E − 01	500
	ESSA	233	1,57E − 02	3,66E − 01	
	GWO	370	1,61E − 03	5,96E − 01	
	MGO	233	6,20E − 03	1,44E + 00	
	PSO	9	9,52E − 04	8,57E − 03	
F14	AVOA	49	1,76E − 03	8,62E − 02	1,000
	ESSA	165	2,51E − 02	4,14E + 00	
	GTO	52	2,86E − 03	1,49E − 01	
	MGO	174	9,49E − 03	1,65E + 00	

ESSA, electro search simulated annealing.

Table 9: D-H Parameters for manipulator [49].

i	t_i	α_i	d_i	θ_i (range of variable)
1	0.50	−90	0	−180–180
2	0.20	90	0	−90–30
3	0.25	−90	0	−90–120
4	0.30	90	0	−90–90
5	0.20	−90	0	−90–90
6	0.20	0	0	−90–90
7	0.10	0	0.05	−30–90

$$A_2 = \begin{bmatrix} \cos\theta_2 & 0 & \sin\theta_2 & t_2 \cdot \cos\theta_2 \\ \sin\theta_2 & 0 & -\cos\theta_2 & t_2 \cdot \sin\theta_2 \\ 0 & 1 & 0 & d_2 \\ 0 & 0 & 0 & 1 \end{bmatrix}, \quad (26)$$

$$A_3 = \begin{bmatrix} \cos\theta_3 & 0 & -\sin\theta_3 & t_3 \cdot \cos\theta_3 \\ \sin\theta_3 & 0 & \cos\theta_3 & t_3 \cdot \sin\theta_3 \\ 0 & -1 & 0 & d_3 \\ 0 & 0 & 0 & 1 \end{bmatrix}, \quad (27)$$

$$A_4 = \begin{bmatrix} \cos\theta_4 & 0 & \sin\theta_4 & t_4 \cdot \cos\theta_4 \\ \sin\theta_4 & 0 & -\cos\theta_4 & t_4 \cdot \sin\theta_4 \\ 0 & 1 & 0 & d_4 \\ 0 & 0 & 0 & 1 \end{bmatrix}, \quad (28)$$

$$A_5 = \begin{bmatrix} \cos\theta_5 & 0 & -\sin\theta_5 & t_5 \cdot \cos\theta_5 \\ \sin\theta_5 & 0 & \cos\theta_5 & t_5 \cdot \sin\theta_5 \\ 0 & -1 & 0 & d_5 \\ 0 & 0 & 0 & 1 \end{bmatrix}, \quad (29)$$

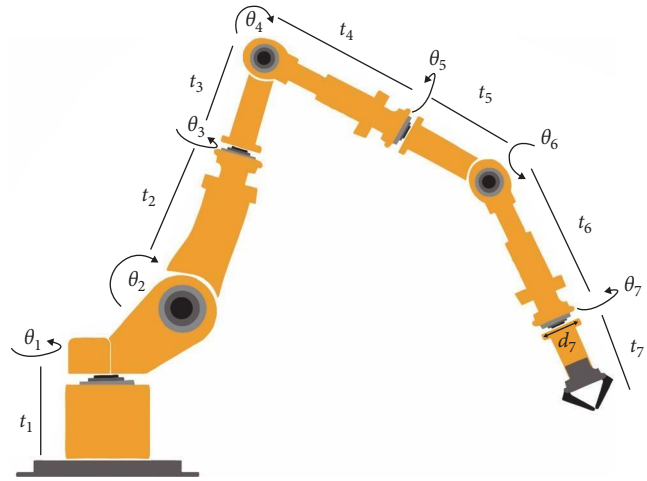

FIGURE 5: 7-DOH serial robotic manipulator.

$$A_6 = \begin{matrix} \cos\theta_6 & -\sin\theta_6 & 0 & t_6 \cdot \cos\theta_6 \\ \sin\theta_6 & \cos\theta_6 & 0 & t_6 \cdot \sin\theta_6 \\ 0 & 0 & 1 & d_6 \\ 0 & 0 & 0 & 1 \end{matrix}, \tag{30}$$

$$A_7 = \begin{matrix} \cos\theta_7 & -\sin\theta_7 & 0 & t_7 \cdot \cos\theta_7 \\ \sin\theta_7 & \cos\theta_7 & 0 & t_7 \cdot \sin\theta_7 \\ 0 & 0 & 1 & d_7 \\ 0 & 0 & 0 & 1 \end{matrix}. \tag{31}$$

The 7-DOF serial manipulator is shown in Figure 5. In the forward kinematic analysis of the 7-DOF serial manipulator, the position of the end effector is determined using Equations (32) and (33) [73].

$${}^0_7T = A_1.A_2.A_3.A_4.A_5.A_6.A_7, \tag{32}$$

$${}^0_7T = \begin{matrix} n_x & s_x & a_x & P_x \\ n_y & s_y & a_y & P_y \\ n_z & s_z & a_z & P_z \\ 0 & 0 & 0 & 1 \end{matrix}, \tag{33}$$

n_x, n_y, n_z is the average vector, s_x, s_y, s_z is the orientation vector, a_x, a_y, a_z is the approximate vector, and P_x, P_y, P_z is the vector giving the end effector position.

5.2. Determination of Objective Function. For the 7-DOF serial robot manipulator, an objective function is needed to identify the end effector's location. The objective function is the function that defines the position errors concerning the locations P_x, P_y, and P_z derived from the forward kinematic analysis. The position errors are the differences between the position obtained due to the seven determined joint angles and the determined position of the end effector. The amount of error is calculated as the root-mean-square error (RMSE) (Equation 34) [74]. As the error rate approaches zero, the end effector of the robot manipulator gets closer to the target position. The proposed ESSA hybrid algorithm estimates joint angles approximating the determined position target.

$$\text{RMSE} = \sqrt{\frac{1}{n}\sum_{i=1}^{n} e_i^2}, \tag{34}$$

$$e = P_j^{\text{I}} - P_j j \in x, y, z, \tag{35}$$

n is the number of arms, e is the error, P^{I} is the target position, and P is the current position.

5.3. 7-DOF Robotic Manipulator Performance. The inverse kinematic problem of a 7-DOF robot manipulator was used to evaluate the proposed hybrid ESSA algorithm's performance. For the solution to the problem, three different target positions were determined. The first target is [−20, 90, 3], the second target is [25, 30, 40], and the last target is [−53, 80, 92]. To reach the specified targets, the manipulators must have certain joint angles. Calculating these angles using metaheuristic algorithms is one of the preferred methods. For this, random angles are initially selected. Then, by solving the inverse kinematic problems, the fitness values are calculated. Thus, the joint angles of the manipulators are found. In this process, the algorithms' computation times, location errors, and standard deviations were calculated. Eight metaheuristic algorithms were used to compare these calculations. These are the PSO, GWO, GA, ESO, ESSA, ASO, ANT, and ABC algorithms. In all algorithms, the population size was set to 20, and the maximum number of iterations was set to 300. The algorithms were run separately 20 times under the same conditions. The objective is to evaluate whether the end effector correctly reaches the determined position. Table 10 shows the angles $(\theta_1^* - \theta_7^*)$, the position of the end effector (P_x, P_y, P_z), and position errors concerning the target points.

In Table 10, the number of iterations that the algorithms reached the first target location, the average processing times per iteration, and total processing times are provided.

Table 10: Number of iterations to reach the first target position and total processing time.

Algorithms	Ave-time (t) (s)	Iteration (i)	Total time ($i \times t$) (s)
PSO	1.00E − 03	265	2.65E − 01
GWO	8.83E − 03	300	2.65E + 00
GA	4.85E − 01	300	7.28E + 00
ESO	4.70E − 03	297	1.40E + 00
ESSA	5.90E − 03	201	1.19E + 00
ASO	1.40E − 03	294	4.12E − 01
ANT	3.60E − 03	296	1.07E + 00
ABC	1.70E − 02	288	4.90E + 00

ESSA, electro search simulated annealing.

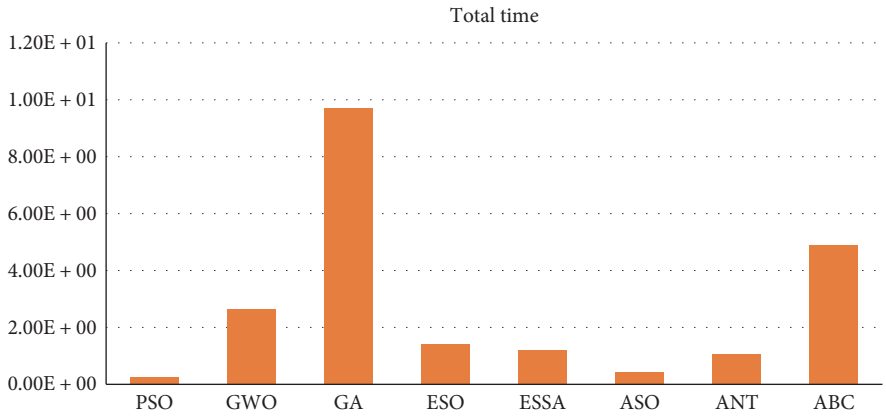

Figure 6: The execution time of the algorithms to reach the first target position.

According to the total processing times obtained, the three fastest algorithms were PSO, ASO, and ESSA, respectively. The ESSA algorithm can be said to have superior performance as it provides full access to the target location, and its calculation time is comparable to the other two algorithms. The comparison of the total computation time of the algorithms is given in Figure 6.

When Table 11 is analyzed, it is observed that the proposed ESSA algorithm reaches all three given targets for the end effector position with zero error. On the other hand, the ASO has a minor location error following the ESSA algorithm. Table 12 shows the average time it took the algorithms one iteration to reach the target position and their standard deviation.

The fact that the standard deviations of the algorithms are minor within the three determined locations indicates the algorithms' ability to solve problems. Although the PSO algorithm reached the result in the shortest time, it was observed that the error rate was higher than the proposed ESSA algorithm. When we look at the ESSA algorithm, it can solve the problem in the same average time as the other metaheuristic algorithms.

Iteration-dependent third target error (−53, 80, and 92) is shown in Figure 7. The error amounts are given in centimeter. When the graph is analyzed, it is observed that the error amount of the ESSA algorithm approaches zero over time and becomes zero. The ASO algorithm was the second algorithm that could calculate the closest position with an error of 2.4469E−14 cm.

Figure 8 demonstrates the positions of the algorithms at the specified target after 300 iterations. The ESSA algorithm is the only one capable of reaching the specified positions of 30, 40, and 35 in the second target with zero error. Subsequently, the ASO and PSO algorithms were the ones that approached this position with the least error.

6. Conclusions and Future Work

To help eliminate local optima and further increase solution accuracy compared to ESO, a new hybrid algorithm proposal has been presented. ESSA has been compared with 10 metaheuristic algorithms. Numerical data shows that ESSA has high-solution accuracy for many unimodal and multimodal functions, proving the proposed ESSA to be effective in global optimization problems. The Friedman test reveals that ESSA has the highest Ave-rank value in global optimization problems, while the Wilcoxon signed-rank test indicates that ESSA's performance is different from other algorithms at a 5% significance level. Moreover, ESSA is also capable of balancing exploration and exploitation. In unimodal functions, ESSA's hybrid structure increases the execution time. However, it completes multimodal functions in the same time frames as others. Complex global optimization problems have been solved using 100, 500, and 1,000-

Table 11: Determined angles to the target point, position, and position error of the end effector (cm).

	Algorithms	θ_1°	θ_2°	θ_3°	θ_4°	θ_5°	θ_6°	θ_7°	$\mathbf{P_x}$	$\mathbf{P_y}$	$\mathbf{P_z}$	Position error (cm)
[−20, 90, 3]	PSO	85.342	30.000	−1.669	−33.038	51.694	60.000	8.057	−20.03	89.94	3.02	6.4664 E− 04
	GWO	34.268	−9.855	82.841	40.524	0.1132	0.691	−0.266	−19.94	89.95	2.94	3.4055 E− 04
	GA	47.176	−3.058	57.883	29.642	13.141	39.608	−20.797	−20.03	90.06	2.96	7.9682 E− 04
	ESO	66.914	−13.140	42.884	41.127	5.8913	33.070	20.621	−18.71	89.38	4.22	1.8820 E− 02
	ESSA	**56.695**	**−0.238**	**80.565**	**49.945**	**−47.448**	**−3.843**	**−23.333**	**−20.00**	**90.00**	**3.00**	**0**
	ASO	80.618	−18.478	31.705	−0.031	59.417	9.358	22.767	−20.00	99.99	2.99	1.0392 E− 14
	ANT	49.984	−38.985	57.405	36.352	36.352	15.299	40.212	−17.54	70.55	5.482	2.5204 E− 02
	ABC	135.272	9.6169	−14.623	14.912	−57.068	59.122	43.240	−20.58	88.53	2.87	1.5882 E− 02
[25, 30, 40]	PSO	7.5612	−10.940	−18.845	90.000	90.00	60.000	−30.000	30.023	40.021	25.007	3.1850 E− 04
	GWO	−35.624	1.2304	43.502	90.000	90.00	−1.690	28.601	29.982	39.998	24.971	3.4055 E− 04
	GA	47.177	−3.058	57.883	29.643	13.142	39.609	−20.798	20.031	90.060	29.577	7.9682 E− 04
	ESO	−89.314	−10.397	12.433	73.572	78.166	30.992	32.469	33.741	43.711	17.727	8.9813 E− 02
	ESSA	**8.2887**	**−40.977**	**28.222**	**83.839**	**66.443**	**34.177**	**55.072**	**30.000**	**40.000**	**25.000**	**0**
	ASO	−82.211	1.4073	97.764	63.815	83.279	−13.358	16.566	30.000	40.000	25.000	1.4443 E− 14
	ANT	−81.018	5.4274	120.00	11.908	60.506	60.000	29.076	22.815	41.103	15.353	7.2557 E− 02
	ABC	11.366	−8.0832	63.192	76.896	−13.117	16.331	10.682	28.639	41.040	24.654	1.7469 E− 02
[−53, 80, 92]	PSO	100.22	19.899	40.158	−53.079	−8.7298	−27.451	5.4795	−52.643	79.586	92.216	3.1850 E− 04
	GWO	179.85	−74.977	−82.166	40.699	23.313	−30.898	46.131	−53.004	80.021	91.969	3.7766 E− 04
	GA	−159.85	−27.649	−83.496	−8.1367	4.5187	−2.4405	33.431	−52.966	79.990	91.972	4.5045 E− 04
	ESO	123.61	−56.157	−30.097	67.119	38.335	−17.621	−2.3528	−52.805	79.754	91.881	3.3590 E− 03
	ESSA	**118.20**	**−65.150**	**18.902**	**58.440**	**−18.847**	**2.6290**	**4.2610**	**−53.000**	**80.000**	**92.000**	**0**
	ASO	113.43	−30.028	−5.3199	39.610	41.541	−59.851	−23.607	−53.000	80.000	92.000	2.4469 E− 14
	ANT	94.569	−20.617	13.377	12.440	45.323	−52.950	−14.486	−38.436	87.712	73.430	4.0143 E− 02
	ABC	−37.803	−10.560	66.344	−42.580	−22.674	−29.974	21.284	−51.358	81.107	93.367	2.4068 E− 02

ESSA, electro search simulated annealing. Bold values indicate the best values in the category.

Table 12: Computation one iteration average time and standard deviation of algorithms.

Algorithms		1. Target position [−20, 90, 3]	2. Target position [25, 30, 40]	3. Target position [53, 80, 92]
PSO	Time (s)	1.00E−03	1.14E−03	1.18E03
	Deviation	4.54E−02	4.40E−02	4.40E02
GWO	Time (s)	8.83E−03	8.71E−03	8.84E−03
	Deviation	2.50E−04	1.50E−04	4.40E04
GA	Time (s)	4.85E−01	4.85E01	4.95E−01
	Deviation	8.14E−02	8.13E02	4.78E−02
ESO	Time (s)	4.70E−03	4.60E03	4.80E−03
	Deviation	7.20E02	4.63E02	6.56E−02
ESSA	Time (s)	5.90E−03	8.75E03	8.74E−03
	Deviation	3.63E02	4.95E02	5.01E−02
ASO	Time (s)	1.40E−03	2.30E03	2.30E−03
	Deviation	4.76E02	4.39E02	4.61E−02
ANT	Time (s)	3.60E−03	2.51E03	3.30E−03
	Deviation	9.00E−03	3.06E02	2.40E−02
ABC	Time (s)	1.70E02	2.70E−03	3.03E−03
	Deviation	5.45E−02	2.05E−03	4.35E−02

ESSA, electro search simulated annealing.

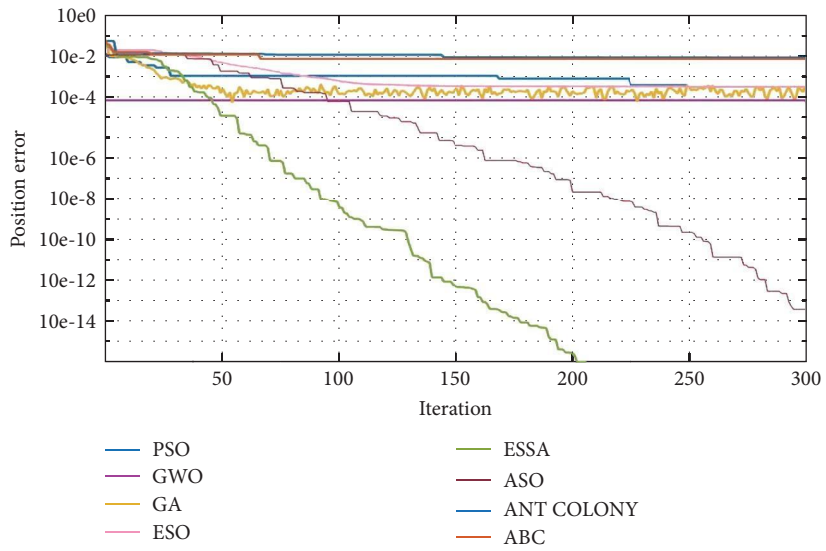

Figure 7: Iteration-dependent third target position error.

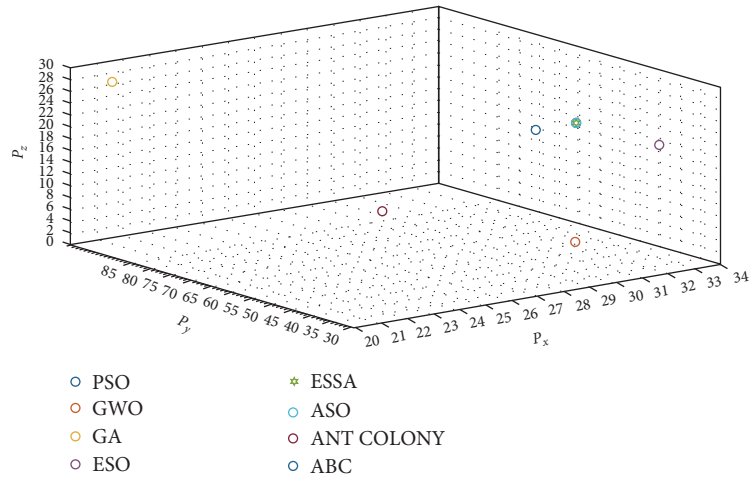

Figure 8: The locations of the algorithms for the second target.

dimensional unimodal and multimodal functions to analyze their performance. Numerical results show that ESSA has the highest Ave-rank value. Finally, the inverse kinematic analysis of a 7-DOF free manipulator has been performed using metaheuristic algorithms. Experimental results demonstrate that ESSA can solve engineering problems efficiently and error free.

In this paper, we make the following contributions:

(1) ESSA uses the strategy of pushing individuals to escape local optima by utilizing the SA algorithm, thus reaching global exploration and achieving solution accuracy.
(2) ESSA effectively solves multidimensional problems.
(3) In medical applications, where a very low-error rate is required, ESSA can reach a complete solution. This demonstrates its highly competitive structure.

However, ESSA is unable to solve global optimization problems in a very short time. The time factor increases when balancing exploration and exploitation. Therefore, in future work, we will continue to improve this capability. We will also apply ESSA to areas such as image analysis and optimizing network coefficients in artificial neural networks.

Data Availability

The data that support the findings of this study are available from the corresponding author upon reasonable request.

Conflicts of Interest

The authors declare that they have no conflicts of interest.

References

[1] F. S. Gharehchopogh, "Quantum-inspired metaheuristic algorithms: comprehensive survey and classification," *Artificial Intelligence Review*, vol. 56, pp. 5479–5543, 2023.
[2] M. Tunay, E. Pashaei, and E. Pashaei, "Hybrid hypercube optimization search algorithm and multilayer perceptron neural network for medical data classification," *Computational Intelligence and Neuroscience*, vol. 2022, Article ID 1612468, 16 pages, 2022.
[3] H. Zamani, M. H. Nadimi-Shahraki, and A. H. Gandomi, "QANA: quantum-based avian navigation optimizer algorithm," *Engineering Applications of Artificial Intelligence*, vol. 104, Article ID 104314, 2021.
[4] F. S. Gharehchopogh and H. Gholizadeh, "A comprehensive survey: whale optimization algorithm and its applications," *Swarm and Evolutionary Computation*, vol. 48, no. 1, pp. 24–24, 2019.
[5] C. Blum and A. Roli, "Metaheuristics in combinatorial optimization: overview and conceptual comparison," *ACM Computing Surveys*, vol. 35, no. 3, pp. 268–308, 2003.
[6] R. E. Bellman, *Adaptive Control Processes: A Guided Tour*, p. 276, Princeton University Press, 2016.
[7] F. S. Gharehchopogh, M. Namazi, L. Ebrahimi, and B. Abdollahzadeh, "Advances in sparrow search algorithm: a comprehensive survey," *Archives of Computational Methods in Engineering*, vol. 30, pp. 427–455, 2023.
[8] D. Izci and S. Ekinci, "A novel hybrid ASO-NM algorithm and its application to automobile cruise control system," in *Proceedings of 2nd International Conference on Artificial Intelligence: Advances and Applications*, G. Mathur, M. Bundele, M. Lalwani, and M. Paprzycki, Eds., pp. 333–343, Springer, Singapore, 2022.
[9] E. Eker, M. Kayri, S. Ekinci, and D. Izci, "A new fusion of ASO with SA algorithm and its applications to MLP training and DC motor speed control," *Arabian Journal for Science and Engineering*, vol. 46, pp. 3889–3911, 2021.
[10] S. Ekinci, D. Izci, E. Eker, and L. Abualigah, "An effective control design approach based on novel enhanced aquila optimizer for automatic voltage regulator," *Artificial Intelligence Review*, vol. 56, pp. 1731–1762, 2023.
[11] D. Izci and S. Ekinci, "A novel improved version of hunger games search algorithm for function optimization and efficient controller design of buck converter system," *e-Prime—Advances in Electrical Engineering, Electronics and Energy*, vol. 2, Article ID 100039, 2022.
[12] D. Izci, S. Ekinci, E. Eker, and A. Demirören, "Multi-strategy modified INFO algorithm: performance analysis and application to functional electrical stimulation system," *Journal of Computational Science*, vol. 64, Article ID 101836, 2022.
[13] S. Ekinci, D. Izci, L. Abualigah, and R. A. Zitar, "A modified oppositional chaotic local search strategy based aquila optimizer to design an effective controller for vehicle cruise control system," *Journal of Bionic Engineering*, vol. 20, pp. 1828–1851, 2023.
[14] M. Yazdandoost, P. Khazaei, S. Saadatian, and R. Kamali, "Distributed optimization strategy for multi area economic dispatch based on electro search optimization algorithm," in *2018 World Automation Congress (WAC)*, pp. 1–6, IEEE, Stevenson, WA, USA, June 2018.
[15] M. Eslami, E. Akbari, S. T. Seyed Sadr, and B. F. Ibrahim, "A novel hybrid algorithm based on rat swarm optimization and pattern search for parameter extraction of solar photovoltaic models," *Energy Science & Engineering*, vol. 10, no. 8, pp. 2689–2713, 2022.
[16] S. Basak, B. Dey, and B. Bhattacharyya, "Uncertainty-based dynamic economic dispatch for diverse load and wind profiles using a novel hybrid algorithm," *Environment Development and Sustainability*, vol. 25, pp. 4723–4763, 2023.
[17] Y. Teekaraman and H. Manoharan, "Implementation of cognitive radio model for agricultural applications using hybrid algorithms," *Wireless Personal Communications*, vol. 127, pp. 505–522, 2022.
[18] S. Nama, A. K. Saha, S. Chakraborty, A. H. Gandomi, and L. Abualigah, "Boosting particle swarm optimization by backtracking search algorithm for optimization problems," *Swarm and Evolutionary Computation*, vol. 79, Article ID 101304, 2023.
[19] P. Chakraborty, S. Nama, and A. K. Saha, "A hybrid slime mould algorithm for global optimization," *Multimedia Tools and Applications*, vol. 82, pp. 22441–22467, 2023.
[20] S. Sharma, A. K. Saha, S. Roy, S. Mirjalili, and S. Nama, "A mixed sine cosine butterfly optimization algorithm for global optimization and its application," *Cluster Computing*, vol. 25, pp. 4573–4600, 2022.
[21] S. K. Sahoo and A. K. Saha, "A hybrid moth flame optimization algorithm for global optimization," *Journal of Bionic Engineering*, vol. 19, pp. 1522–1543, 2022.
[22] S. Chakraborty, S. Sharma, A. K. Saha, and S. Chakraborty, "SHADE–WOA: a metaheuristic algorithm for global optimization," *Applied Soft Computing*, vol. 113, Part A, Article ID 107866, 2021.

[23] D. Izci, S. Ekinci, and H. L. Zeynelgil, "Controlling an automatic voltage regulator using a novel Harris hawk and simulated annealing optimization technique," *Advanced Control for Applications, Engineering and Industrial Systems*, Article ID e121, 2023.

[24] D. Izci, S. Ekinci, and B. Hekimoğlu, "Fractional-order PID controller design for buck converter system via hybrid lévy flight distribution and simulated annealing algorithm," *Arabian Journal for Science and Engineering*, vol. 47, pp. 13729–13747, 2022.

[25] S. Ekinci, D. Izci, and B. Hekimoğlu, "Optimal FOPID speed control of DC motor via opposition-based hybrid manta ray foraging optimization and simulated annealing algorithm," *Arabian Journal for Science and Engineering*, vol. 46, pp. 1395–1409, 2021.

[26] H. Mohammadzadeh and F. S. Gharehchopogh, "A multi-agent system based for solving high-dimensional optimization problems: a case study on email spam detection," *International Journal of Communication Systems*, vol. 34, no. 3, Article ID e4670, 2021.

[27] J. Kennedy and R. Eberhart, "Particle swarm optimization," in *Proceedings of ICNN'95—International Conference on Neural Networks*, pp. 1942–1948, IEEE, Perth, WA, Australia, November 1995.

[28] W. Zhao, L. Wang, and Z. Zhang, "A novel atom search optimization for dispersion coefficient estimation in groundwater," *Future Generation Computer Systems*, vol. 91, pp. 601–610, 2019.

[29] K. M. Passino, "Biomimicry of bacterial foraging for distributed optimization and control," *IEEE Control Systems Magazine*, vol. 22, no. 3, pp. 52–67, 2002.

[30] S. Mirjalili, S. M. Mirjalili, and A. Lewis, "Grey wolf optimizer," *Advances in Engineering Software*, vol. 69, pp. 46–61, 2014.

[31] D. Di Caprio, A. Ebrahimnejad, H. Alrezaamiri, and F. J. Santos-Arteaga, "A novel ant colony algorithm for solving shortest path problems with fuzzy arc weights," *Alexandria Engineering Journal*, vol. 61, no. 5, pp. 3403–3415, 2022.

[32] D. Karaboga, B. Gorkemli, C. Ozturk, and N. Karaboga, "A comprehensive survey: artificial bee colony (ABC) algorithm and applications," *Artificial Intelligence Review*, vol. 42, pp. 21–57, 2014.

[33] D. S. Weile and E. Michielssen, "Genetic algorithm optimization applied to electromagnetics: a review," *IEEE Transactions on Antennas and Propagation*, vol. 45, no. 3, pp. 343–353, 1997.

[34] H. Shayanfar and F. S. Gharehchopogh, "Farmland fertility: a new metaheuristic algorithm for solving continuous optimization problems," *Applied Soft Computing*, vol. 71, pp. 728–746, 2018.

[35] B. Abdollahzadeh, F. S. Gharehchopogh, and S. Mirjalili, "African vultures optimization algorithm: a new nature-inspired metaheuristic algorithm for global optimization problems," *Computers & Industrial Engineering*, vol. 158, Article ID 107408, 2021.

[36] B. Abdollahzadeh, F. Soleimanian Gharehchopogh, and S. Mirjalili, "Artificial gorilla troops optimizer: a new nature-inspired metaheuristic algorithm for global optimization problems," *International Journal of Intelligent Systems*, vol. 36, no. 10, pp. 5887–5958, 2021.

[37] B. Abdollahzadeh, F. S. Gharehchopogh, N. Khodadadi, and S. Mirjalili, "Mountain gazelle optimizer: a new nature-inspired metaheuristic algorithm for global optimization problems," *Advances in Engineering Software*, vol. 174, Article ID 103282, 2022.

[38] M. Khishe and M. R. Mosavi, "Chimp optimization algorithm," *Expert Systems with Applications*, vol. 149, Article ID 113338, 2020.

[39] M. H. Nadimi-Shahraki and H. Zamani, "DMDE: diversity-maintained multi-trial vector differential evolution algorithm for non-decomposition large-scale global optimization," *Expert Systems with Applications*, vol. 198, Article ID 116895, 2022.

[40] B. Wang, L. Liu, Y. Li, and M. Khishe, "Robust grey wolf optimizer for multimodal optimizations: a cross-dimensional coordination approach," *Journal of Scientific Computing*, vol. 92, no. 3, Article ID 110, 2022.

[41] R. A. Rutenbar, "Simulated annealing algorithms: an overview," *IEEE Circuits and Devices Magazine*, vol. 5, no. 1, pp. 19–26, 1989.

[42] A. Tabari and A. Ahmad, "A new optimization method: electro-search algorithm," *Computers & Chemical Engineering*, vol. 103, pp. 1–11, 2017.

[43] R. Köker, C. Öz, T. Çakar, and H. Ekiz, "A study of neural network based inverse kinematics solution for a three-joint robot," *Robotics and Autonomous Systems*, vol. 49, no. 3-4, pp. 227–234, 2004.

[44] M. Ayyıldız and K. Çetinkaya, "Comparison of four different heuristic optimization algorithms for the inverse kinematics solution of a real 4-DOF serial robot manipulator," *Neural Computing and Applications*, vol. 27, pp. 825–836, 2016.

[45] J. Vaishnavi, B. Singh, A. Vijayvargiya, and R. Kumar, "Inverse kinematics solution for 5-DoF robotic manipulator using meta-heuristic techniques," in *2021 International Conference on Industrial Electronics Research and Applications (ICIERA)*, pp. 1–6, IEEE, New Delhi, India, December 2021.

[46] N. Rokbani, B. Neji, M. Slim, S. Mirjalili, and R. Ghandour, "A multi-objective modified PSO for inverse kinematics of a 5-DOF robotic arm," *Applied Sciences*, vol. 12, no. 14, Article ID 7091, 2022.

[47] A. T. Hasan, A. M. S. Hamouda, N. Ismail, and H. M. A. A. Al-Assadi, "An adaptive-learning algorithm to solve the inverse kinematics problem of a 6 D.O.F serial robot manipulator," *Advances in Engineering Software*, vol. 37, no. 7, pp. 432–438, 2006.

[48] B. Nyong-Bassey and A. Epemu, "Inverse kinematics analysis of novel 6-DOF robotic arm manipulator for oil and gas welding using meta-heuristic algorithms," *International Journal on Robotics, Automation and Sciences Articles*, vol. 4, pp. 13–22, 2022.

[49] S. Dereli and R. Köker, "A meta-heuristic proposal for inverse kinematics solution of 7-DOF serial robotic manipulator: quantum behaved particle swarm algorithm," *Artificial Intelligence Review*, vol. 53, pp. 949–964, 2020.

[50] T. T. Nguyen, T. N. Bui, W. Dai, T. V. Nguyen, and L. N. Tao, "Apply some meta-heuristic algorithms to solve inverse kinematic problems of a 7-DoFs manipulator robot," *International Journal of Mechanical Engineering and Robotics Research*, vol. 10, no. 9, pp. 498–504, Sep. 2021.

[51] A. S. J. Alexis, M. C. E. Alejandro, S. G. F. Arturo, R. C. R. Gustavo, P. F. E. Alfredo, and V. C. Valentin, "Particle swarm optimization for inverse kinematics solution and trajectory planning of 7-DOF and 8-DOF robot manipulators based on unit quaternion representation," *Journal of Applied Engineering Science*, vol. 19, no. 3, pp. 592–599, 2021.

[52] S. Kirkpatrick, C. D. Gelatt, and M. P. Vecchi, "Optimization by simulated annealing," *Science*, vol. 220, no. 4598, pp. 671–680, 1983.

[53] S. Ozturk, L. Aydin, N. Kucukdogan, and E. Celik, "Optimization of lapping processes of silicon wafer for photovoltaic applications," *Solar Energy*, vol. 164, pp. 1–11, 2018.

[54] H. Ahonen, A. G. de Alvarenga, and A. R. S. Amaral, "Simulated annealing and tabu search approaches for the corridor allocation problem," *European Journal of Operational Research*, vol. 232, no. 1, pp. 221–233, 2014.

[55] I. H. Cizmeci and A. A. Altun, "Improved electro search algorithm with intelligent controller control system: ESPID algorithm," *Intelligent Automation & Soft Computing*, vol. 35, no. 3, pp. 2555–2572, 2023.

[56] S. B. Joseph, E. G. Dada, A. Abidemi, D. O. Oyewola, and B. M. Khammas, "Metaheuristic algorithms for PID controller parameters tuning: review, approaches and open problems," *Heliyon*, vol. 8, no. 5, Article ID e09399, 2022.

[57] K. J. A˚ström and P. R. Kumar, "Control: a perspective," *Automatica*, vol. 50, no. 1, pp. 3–43, 2014.

[58] R. H. M. Aly, K. H. Rahouma, and A. I. Hussein, "Design and optimization of PID controller based on metaheuristic algorithms for hybrid robots," in *2023 20th Learning and Technology Conference (L&T)*, pp. 85–90, IEEE, Jeddah, Saudi Arabia, January 2023.

[59] C. Zhao and L. Guo, "PID controller design for second order nonlinear uncertain systems," *Science China Information Sciences*, vol. 60, Article ID 022201, 2017.

[60] J. G. Ziegler and N. B. Nichols, "Optimum settings for automatic controllers," *Journal of Fluids Engineering*, vol. 64, no. 8, pp. 759–765, 1942.

[61] G. H. Cohen and G. A. Coon, "Theoretical consideration of retarded control," *Journal of Fluids Engineering*, vol. 75, no. 5, pp. 827–834, 1953.

[62] Z.-Y. Nie, Q.-G. Wang, M. Wu, and Y. He, "Tuning of multi-loop PI controllers based on gain and phase margin specifications," *Journal of Process Control*, vol. 21, no. 9, pp. 1287–1295, 2011.

[63] Y. Li, K. H. Ang, and G. C. Y. Chong, "Patents, software, and hardware for PID control: an overview and analysis of the current art," *IEEE Control Systems Magazine*, vol. 26, no. 1, pp. 42–54, 2006.

[64] T.-J. Ren, T.-C. Chen, and C.-J. Chen, "Motion control for a two-wheeled vehicle using a self-tuning PID controller," *Control Engineering Practice*, vol. 16, no. 3, pp. 365–375, 2008.

[65] C. Zhang, T. Peng, C. Li, W. Fu, X. Xia, and X. Xue, "Multiobjective optimization of a fractional-order PID controller for pumped turbine governing system using an improved NSGA-III algorithm under multiworking conditions," *Complexity*, vol. 2019, Article ID 5826873, 18 pages, 2019.

[66] M. Daradkeh, L. Abualigah, S. Atalla, and W. Mansoor, "Scientometric analysis and classification of research using convolutional neural networks: a case study in data science and analytics," *Electronics*, vol. 11, no. 13, Article ID 2066, 2022.

[67] J. J. Liang, B. Qu, and P. N. Suganthan, "Problem definitions and evaluation criteria for the CEC, special session and competition on single objective real-parameter numerical optimization," Technical Report 201311, 2013, Computational Intelligence Laboratory, Zhengzhou University, Nanyang Technological University, Zhengzhou, Singapore, 2014.

[68] F. Karami and A. B. Dariane, "A review and evaluation of multi and many-objective optimization: methods and algorithms," *Global Journal of Ecology*, vol. 7, no. 2, pp. 104–119, 2022.

[69] W. W. Daniel, *Applied Nonparametric Statistics*, PWS-Kent Publishing Company, Boston, 1990.

[70] F. Wilcoxon, "Individual comparisons by ranking methods," *Biometrics Bulletin*, vol. 1, no. 6, pp. 80–83, 1945.

[71] T. Dewi, S. Nurmaini, P. Risma, Y. Oktarina, and M. Roriz, "Inverse kinematic analysis of 4 DOF pick and place arm robot manipulator using fuzzy logic controller," *International Journal of Electrical and Computer Engineering (IJECE)*, vol. 10, no. 2, pp. 1376–1386, 2020.

[72] T. P. Singh, P. Suresh, and S. Chandan, "Forward and inverse kinematic analysis of robotic manipulators forward and inverse kinematic analysis of robotic manipulators," *International Research Journal of Engineering and Technology (IRJET)*, vol. 4, no. 2, pp. 1372–1382, 2017.

[73] Y. Cui, P. Shi, and J. Hua, "Kinematics analysis and simulation of a 6-DOF humanoid robot manipulator," in *2010 2nd International Asia Conference on Informatics in Control, Automation and Robotics (CAR 2010)*, vol. 2, pp. 246–249, IEEE, Wuhan, China, March 2010.

[74] T. Chai and R. R. Draxler, "Root mean square error (RMSE) or mean absolute error (MAE)?—arguments against avoiding RMSE in the literature," *Geoscientific Model Development*, vol. 7, no. 3, pp. 1247–1250, 2014.